

**A PARITY VIOLATION
TRANSMISSION EXPERIMENT
FOR UNDERGRADUATE
LABORATORIES**

By

Levi Kennel

A thesis submitted in partial fulfillment of the
requirements for the degree of

Bachelor of Science

Houghton University

May 2024

Signature of Author.....

Department of Physics
May 3, 2024

.....

Dr. Mark Yuly
Professor of Physics
Research Supervisor

.....

Dr. Katrina Koehler
Assistant Professor of Physics

**A PARITY VIOLATION TRANSMISSION
EXPERIMENT FOR UNDERGRADUATE
LABORATORIES**

By

Levi Kennel

Submitted to the Department of Physics
on May 3, 2024, in partial fulfillment of the
requirement for the degree of
Bachelor of Science

Abstract

Because there are currently no published weak interaction parity violation experiments specifically for undergraduate laboratories, a simple parity violation experiment is being developed using circularly polarized gamma rays. A ^{60}Co source will be placed on one side of an electromagnet, so that the circularly polarized gamma rays emitted opposite the beta particles will pass through the electromagnet. A NaI detector detects the number of gamma rays that pass through the electromagnet, and a silicon detector detects in coincidence beta particles opposite the gamma rays. The number of $\gamma\beta$ coincidence events will be measured when the electromagnet is polarized both parallel and antiparallel to the gamma rays — an asymmetry between the number of coincidence events for each orientation would show that parity is violated.

Thesis Supervisor: Dr. Mark Yuly

Title: Professor of Physics

TABLE OF CONTENTS

Chapter 1: The History of Parity Violation Experiments	5
1.1. The Phenomenon of Parity Violation	5
1.2. Invention of Apparatus	7
1.3. History and Development of Parity Violation Experiments	9
1.4. Motivation for Developing a Parity Violation Experiment	14
1.5. Introduction of the Experiment at Houghton University	15
Chapter 2: Theory of Parity Violation	18
2.1. Theory Overview	18
2.2. Beta Decay of ^{60}Co	18
2.3. Gamma Transmission Asymmetry Calculation	25
Chapter 3: Experiment	30
3.1. Experimental Overview	30
3.2. Electromagnet	30
3.3. Detectors	37
3.3.1. NaI Crystal Detector, Light Guide, PMT, and Base	37
3.3.2. Silicon Detector	40
3.4. Electronics	40
Chapter 4: Conclusions	42
<i>Appendix A : SMath File</i>	44
<i>Appendix B : FemtoDAQ Python Code</i>	45
<i>Appendix C : Analysis Codes</i>	51

TABLE OF FIGURES

Figure 1. Axis inversion process for a parity transformation.....	6
Figure 2. Original diagram of Wu’s experimental apparatus.....	8
Figure 3. Wu’s original experimental results.....	10
Figure 4. Goldhaber et al. transmission experimental apparatus.....	11
Figure 5. Goldhaber et al. scattering experimental apparatus.....	13
Figure 6. Lundby et al. experimental apparatus.....	14
Figure 7. Simplified diagram of the Houghton University experiment.....	16
Figure 8. Energy level diagram of ^{60}Co	19
Figure 9. Quantization of the z-component of angular momentum.....	19
Figure 10. Conservation of the z-component of angular momentum.....	20
Figure 11. Two possible particle spins and directions of momenta.....	22
Figure 12. Mirrored ^{60}Co decays showing impossible “configurations”.....	23
Figure 13. The two decay configurations without antineutrinos.....	24
Figure 14. Gamma transmission through polarized magnet core.....	25
Figure 15. Plot of predicted gamma asymmetry as a function of core thickness.....	28
Figure 16. Plot of predicted gamma transmission versus core thickness.....	28
Figure 17. Plot of predicted relative uncertainty versus core thickness.....	29
Figure 18. Block diagram of Houghton transmission experiment.....	31
Figure 19. Vector field representation of the simulation of the magnet field.....	33
Figure 20. CAD drawing of electromagnet yoke.....	34
Figure 21. Picture of completed (but not yet painted) electromagnet yoke.....	35
Figure 22. AutoCAD design of bobbin which housed the magnet’s coil.....	35
Figure 23. Apparatus for winding coil onto bobbin.....	36
Figure 24. Completed electromagnet assembly.....	37
Figure 25. Block diagram of energy spectra test circuit.....	39
Figure 26. Energy spectrum of ^{137}Cs	40

Chapter 1

THE HISTORY OF PARITY VIOLATION EXPERIMENTS

1.1. *The Phenomenon of Parity Violation*

Every process in our universe is in some sense the result of one or more of the four fundamental forces: strong nuclear, electromagnetic, gravitational, and weak nuclear force. At first glance, it may appear that each force conserves parity; this means that it would be impossible to determine experimentally if the coordinate axes were inverted as shown in Figure 1. By the 1950's, parity violation had been observationally confirmed for the gravitational, electromagnetic, and strong nuclear forces. It was therefore assumed to also be true of the weak nuclear force, even though this had not been tested. Very quickly, parity conservation within all fundamental forces became accepted as (almost) fact [1]; it was a beautiful theory, and beautiful theories are easy to believe. Unfortunately, that does not make them correct. While not everyone was so convinced, ideas challenging parity conservation found support hard to come by. In 1929 for example, Hermann Weyl introduced a hypothesis [2] challenging the idea of parity conservation, but in 1933 Wolfgang Pauli dismissed this idea [3] simply on the basis that it would violate parity conservation. As it turned out, this was exactly the way that parity would be violated in the weak nuclear force.

The question of parity conservation in weak interactions remained a subject that few were willing to tackle until the 1950s. It seemed the issue had faded into the background, when the discovery of several new particles and the "tau-theta" puzzle brought it to the forefront of issues to address. While the tau and theta particles (now known as the K^+ particle) were measured to have identical masses and decay lifetimes, they had differing parities [4]. To conserve parity, these had to be two different particles. Physicists struggled to reconcile the issue under the standing theory, however no two-particle hypothesis was able to explain the differing parity measurements.

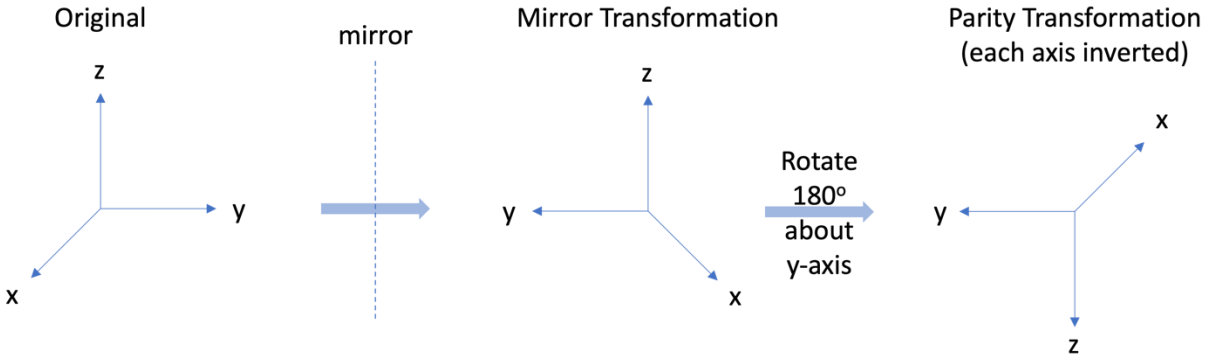


Figure 1. Axis inversion process for a parity transformation. A parity transformation is equivalent to a mirror transformation followed by a rotation.

Finally, at the Sixth Annual Rochester Conference in April 1956, the possibility of parity violation was discussed by the world’s top physicists. The idea was brought to the group by Martin Block and Richard Feynman [5], whose discussion spurred the minds of many into motion. Tsung Dao Lee and Chen Ning Yang were among the physicists at the conference and had been heading up theoretical research into the tau-theta puzzle. Soon after the conference, they met to discuss the idea that parity was violated in the weak nuclear force [1]; it did not take them long to realize that parity conservation had never been verified experimentally in the weak nuclear force, and by June 22, 1956 they had submitted a paper exploring this possibility. Their paper, titled “Question of Parity Conservation in Weak Interactions” [6], was published in October of 1956, highlighting different ways that parity conservation could be tested. In their paper, Lee and Yang described how none of the previous experiments studying beta decay measured data relevant to determining whether parity was conserved in this process. They proposed several different experiments, one of which involved measuring the number of the electrons emitted at certain angles from a polarized parent nucleus during beta decay. If the electrons from a parent nucleus with an upwards oriented spin axis are emitted at angle θ from the spin axis, then reversing the direction of the parent nucleus spin results in an inversion of the parent nucleus spin axis. This inversion means the electrons would then be emitted at angle $180 - \theta$ from the spin axis. Any difference in the number of electrons emitted at angle θ from the spin axis of the versus angle $180 - \theta$ from the spin axis in the reversed spin system would prove that parity

is violated. According to Lee and Yang, another experimental option [6] was to measure the circular polarization of the gamma rays emitted antiparallel to the beta particles when decaying into a “stretched state.” If a difference between the number of gamma rays with right versus left-handed circular polarizations could be measured, parity would be violated. At that time it was believed that circular polarization of gamma rays could not be measured, but later experiments successfully used this measurement; this is the method used in this thesis.

These ideas sent shock waves throughout the physics community; while many experimental physicists raced to be the first to determine whether parity was indeed violated, some scoffed at the idea; most notable were Richard Feynman and Wolfgang Pauli. Feynman bet Norman Ramsay \$50 to \$1 against Lee and Yang’s theory (and lost), while Pauli wrote: “I do not believe that the Lord is a weak left-hander, and I am ready to bet a very large sum that the experiments will give symmetric results” [7] — news of Wu’s results confirming parity violation reached him soon after in a stroke of ironic humor.

1.2. Invention of Apparatus

While Lee and Yang were developing their paper proposing these experiments, they consulted Chien Shiung Wu [1] regarding possible experiments to test their new hypothesis. Wu was a colleague of Lee’s at Columbia University, and a leader in the field of beta decay. When she heard of Lee and Yang’s ideas, she immediately began working on an experiment that would test parity conservation. Wu’s experimental apparatus is shown in Figure 2. Following the ideas that Lee and Yang outlined in their paper, Wu developed an experiment to measure the angular distribution of betas emitted from an oriented ^{60}Co nucleus [8], selected because it can be polarized by the Rose-Gorter method and because of the nature of its beta decay. The Rose-Gorter method requires the source to be subjected to a magnetic field under extremely low temperatures. The magnetic field aligns the ^{60}Co nuclei, while the cryostat reduces the energies of the nuclei enough for them to stay in the polarized state with little variation. Gamma events were measured by an equatorial and a polar NaI crystal detector, and the difference in count rates allowed the degree of polarization of the source nuclei to be measured. The rate of beta events was measured by an anthracene crystal

detector. The magnetic field was achieved using an electromagnet so that the ^{60}Co nuclei could be polarized in two opposite directions; a measured difference in the rate of beta events between opposite polarizations of the source meant that parity was violated.

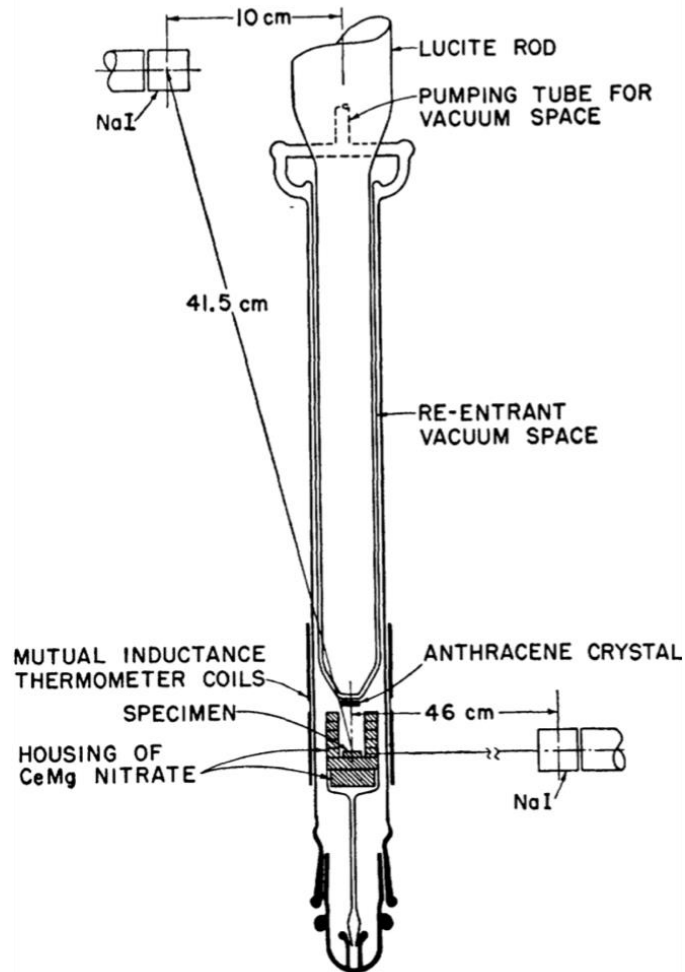


Figure 2. Original diagram of Wu's experimental apparatus. The drawing shows the lower part of the cryostat, which is the essential piece in polarizing the ^{60}Co source. The anthracene crystal counts beta particles as they are emitted from the source. Measurements were taken when the source was polarized both upwards and downwards. Also shown are the two sodium iodide (NaI) detectors, which are responsible for measuring the equatorial and polar counting rates of gamma rays from the source (an indication of the degree of source polarization). A difference between beta counting rates when the source is polarized upwards versus downwards shows that parity is violated. Figure taken from Ref. [8].

Only a few short months after Lee and Yang's paper was officially published (October 1956), Wu published the first experimental data showing that parity was violated in the weak

nuclear force [8]. Figure 3 shows counting rate data from the anthracene detector and both NaI detectors over time. The plot shows an asymmetry between beta count rates when the source was polarized in opposite directions; this asymmetry disappears as the source becomes less polarized. The degree of source polarization can be determined from the gamma anisotropy plot, which is proportional to the difference in counting rates measured by the equatorial and polar gamma detectors over time; the less asymmetry shown between equatorial and polar counting rates, the less polarized the source it. The data confirm an asymmetry in the number of beta events in oppositely polarized nuclei, which in turn confirms parity is violated. This experimental breakthrough led many experiments to follow in the so-called “parity revolution.”

1.3. History and Development of Parity Violation Experiments

While Wu’s experiment led the way for testing parity conservation, it was not the only way to study this phenomenon. In their paper, Lee and Yang mentioned that parity violation could also be tested using the circularly polarized gamma rays that resulted from beta decay of certain nuclei [6]. At the time, Lee and Yang dismissed this method as impossible due to difficulty in measuring the circular polarization of gamma rays. Lee and Yang’s dismissal of this method proved preemptive however, as the Goldhaber et al. experiment demonstrated [9]. Unlike Wu’s experiment, the Goldhaber et al. experiment focused on measuring the circular polarization of the gamma rays emitted opposite the electron and neutrino during beta decay. This experiment utilized the transmission method to measure the circularly polarized bremsstrahlung emitted from the beta particles colliding with lucite. The electromagnet was oriented below the source as seen in Figure 4, and was able to switch directions to orient the electron spins of the magnet upwards or downwards. The right- and left-handed bremsstrahlung gamma rays scattered differently when passing through the upwards or downwards electron spin orientations in the magnet. Since in this experiment the gamma rays were right-handed more than left-handed, a difference in the number of gamma rays passing through the electromagnet was measured when the magnet was polarized upwards versus downwards. These measurements were ultimately what established the fixed helicity of the neutrino. The parity violation experiment at Houghton

University also utilizes the transmission method for measuring circularly polarized gamma rays.

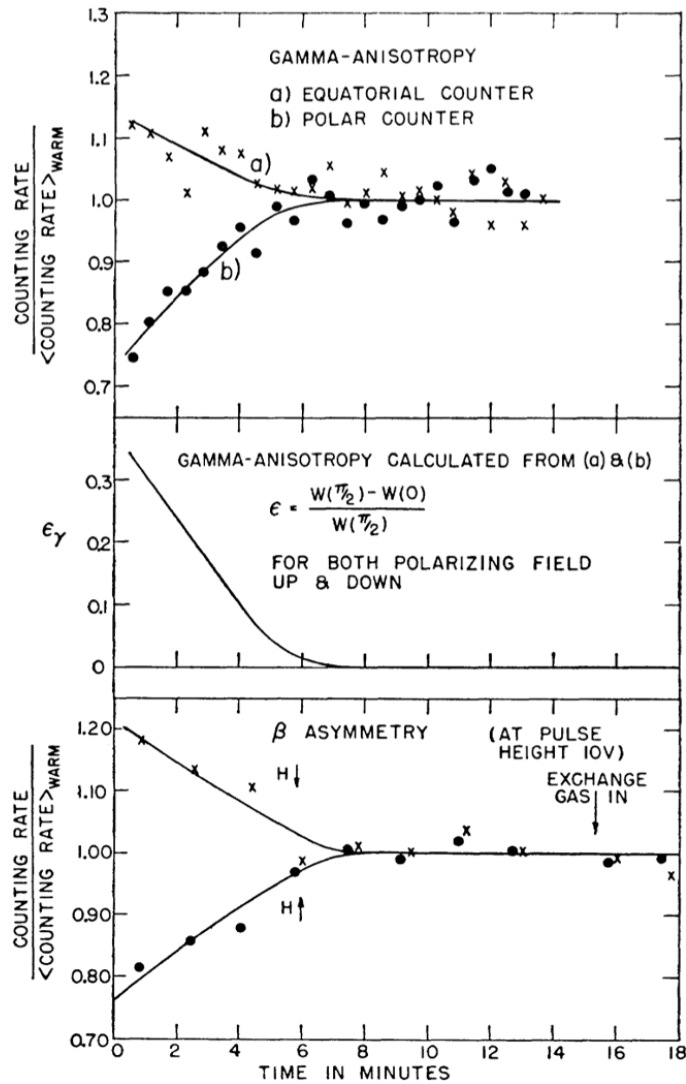


Figure 3. Wu's original experimental results. The top plot shows the counting rate of both the equatorial and polar gamma counters over time (in minutes). The ^{60}Co source started polarized and depolarized over the next minutes – the amount of polarization can be estimated by the magnitude of asymmetry between the two counters. This is because a polarized source will emit gammas disproportionately in certain directions, whereas an unpolarized source is equally likely to emit gammas in any direction. After roughly eight minutes the source was fully depolarized, and the counting rates between the two gamma counters became equal. The middle plot shows the difference between the a) and b) counting rates in the first plot over time divided by $W(\pi/2)$, or the counting rate in the 90° detector. The bottom plot shows the counting rate of beta particles when the source was polarized up versus when the source was polarized down. Again, rates were measured between the two as the source depolarized. Figure taken from Ref. [8].

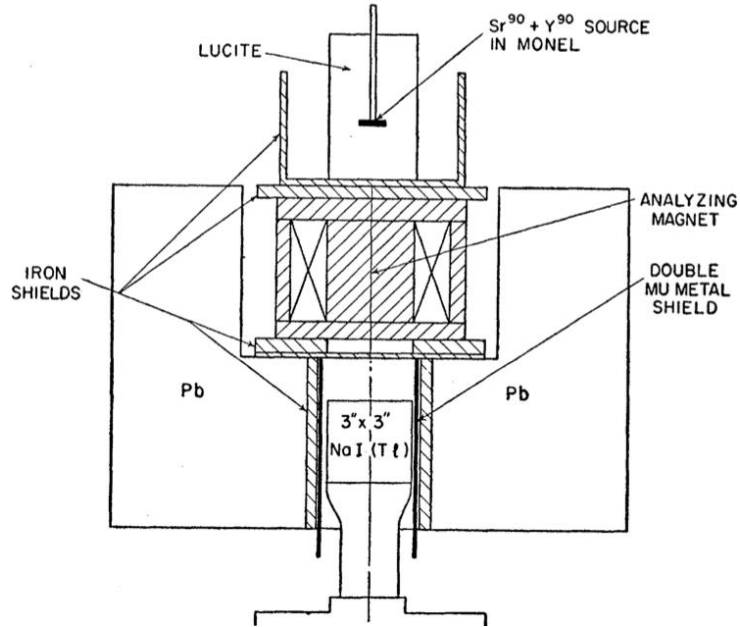


Figure 4. Goldhaber et al. transmission experimental apparatus. When the source decayed, beta particles collided with the lucite nuclei, emitting bremsstrahlung (electromagnetic radiation with the same properties as gamma rays). These “gamma rays” traveled through the electromagnet; some are scattered out and some travel through and hit the NaI detector. These gamma rays had angular momentum perpendicular to their linear momentum, which caused them to travel with a helical motion. The dipoles in the magnet were aligned either parallel or antiparallel to the linear momentum of the gamma rays. If the dipoles were aligned antiparallel, they scattered a right-handed helix gamma differently than a left-handed helix, and vice versa if the dipoles were aligned parallel. If there are an equal number of gammas with a right helix as with a left helix, there will be no measurable difference in counts with the dipoles aligned upwards versus downwards. A measurable difference in counts between the two dipole orientations means that the gammas spin one way more than the other, thus violating parity. Figure takes from Ref [9].

Another experiment by Goldhaber et al. [10] measured the helicity of the neutrino. When a nucleus (in this case ^{152}Eu) decays via electron capture, it emits a neutrino and a gamma ray directly opposite one another. Due to conservation of momentum and angular momentum, the neutrino and the gamma ray must have the same helicity, meaning they have the same relative orientation of their linear momentum and spin — either aligned or antialigned. This means that a measurement of the circular polarization of the gamma rays would directly indicate the helicity of the neutrinos. To obtain this measurement, Goldhaber et al. utilized the scattering method to measure the polarization of the gamma rays emitted opposite of neutrinos in electron capture of ^{152}Eu . Like the previous Goldhaber et al. experiment, in this

experiment gamma rays with different circular polarizations scattered differently from the electromagnet – rather than measuring the number of transmitted gamma rays, however, this experiment measured the number of scattered gamma rays to determine the circular polarization of the gamma rays and in turn the neutrino. Figure 5 shows how gamma rays scattered by the magnet were re-directed back to the NaI detector with an Sm_2O_3 scattering ring. The data collected from this experiment was consistent with the hypothesis that the neutrino was polarized with a negative helicity 100% of the time. Since there is no differentiation between the neutrinos in electron capture and β^+ decay, they concluded that these neutrinos would also be characterized with a negative helicity 100% of the time. Thus, they concluded, the antineutrinos emitted during β^- decay (naturally possessing qualities opposite those of the neutrino) were emitted with positive helicity 100% of the time. This was a shocking result, as it was contrary to the behavior of every other known particle — a neutrinos spin always points opposite its momentum, which means neutrinos are always left-handed. This is what drives parity violation.

Another set of parity violation experiments were carried out by Schopper et al. [11]. Like the Goldhaber et al. transmission experiment, one of these experiments used the absorption method to measure the asymmetry in the number of right versus left-handed circularly polarized gamma rays. Again, an electromagnet was used to filter gamma rays emitted opposite the beta particle; the right and left circular polarizations of the gamma rays were scattered differently by the parallel and antiparallel electron spin orientations of the electromagnet. The Schopper et al. paper is useful because it explained in detail how the transmission rates of the two different gamma ray circular polarizations were calculated based on the Compton scattering of the gamma rays with polarized electrons in the electromagnet core. This was then used to calculate expected asymmetry values for magnets of varying dimensions.

The Lundby et al. experiment [12] is most closely related to the experiment being developed at Houghton. Similar to the Goldhaber et al. and the Schopper et al. transmission experiments, the Lundby et al. apparatus shown in Figure 6 used gamma transmission through an iron electromagnet to measure the circular polarization of gamma rays.

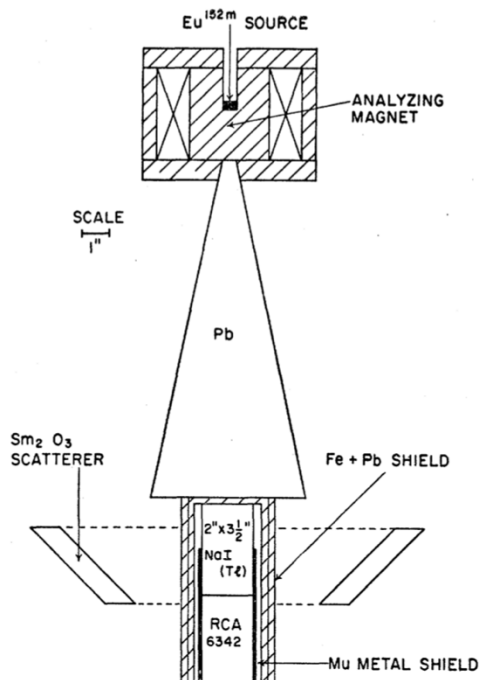


Figure 5. Goldhaber et al. scattering experimental apparatus. Circularly polarized gamma rays were emitted directly opposite the neutrinos as the ^{152}Eu underwent electron capture. These gamma rays traveled into the electromagnet, whose magnetic dipoles could be aligned upwards or downwards. As the gamma rays traveled through the electromagnet, some were Compton scattered and some passed directly through without scattering. The gamma rays that Compton scattered were directed using the Sm_2O_3 scatterer ring towards the center of the ring, where the gamma counting rate was measured by the NaI detector. The number of gamma rays scattered depended on their circular polarization and the alignment of the electromagnet, which caused different counting rates based on the alignment of the magnetic dipoles. The experiment showed that the gamma rays had a negative (left-handed) helicity, which directly corresponded to the helicity of the neutrino due to conservation of momentum and angular momentum. Thus, Goldhaber et al. concluded that an antineutrino must have a positive (right-handed) helicity. Figure taken from Ref. [10].

These gamma rays were emitted opposite the electrons in the beta decay of a ^{60}Co source; an anthracene detector was used to count the emitted betas, and a NaI detector was used to count the gamma rays that were not scattered by the electromagnet. The two detectors verified coincidence events for the beta-gamma pairs, and the number of coincidence events was counted for the parallel and antiparallel magnetic field orientations. The difference between the two counting rates depended on the dipole orientation of the electromagnet, thus showing the gamma rays' bias to a right-handed circular polarization. This experiment proved effective in measuring the asymmetry between the number of gamma rays emitted

with a right-handed or left-handed circular polarization from the beta decay of ^{60}Co , while simplifying the processes utilized in other experiments.

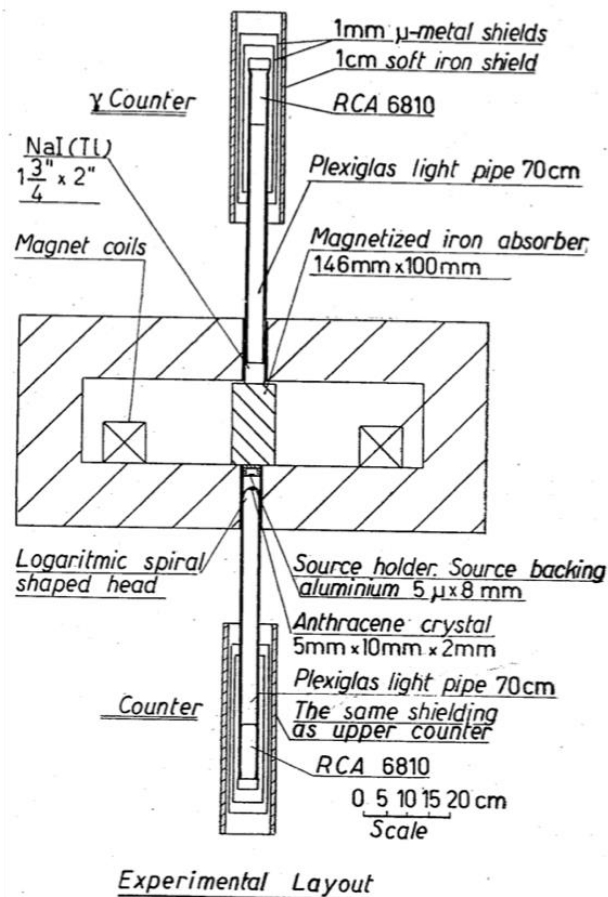


Figure 6. Lundby et al. experimental apparatus. This experiment is similar to the current experiment at Houghton. When the electromagnet was on, the electron dipoles in the steel core were polarized in the same direction, meaning the spins of the electrons were in the same direction. Gamma rays were “shot” through the electromagnet from the ^{60}Co source — these gamma rays had either right or left-handed circular polarization if they were emitted in coincidence with the detected beta at 180° . The right and left circularly polarized gamma rays scattered differently from the two different electron spin orientations. Gamma counts were measured by the NaI crystal detector, and verified if there was an electron measured in coincidence by the Anthracene crystal detector. The plexiglass light guides were necessary to carry the crystal light pulses to the PMTs beyond the reach of the electromagnet’s field. Figure taken from Ref. [12].

1.4. Motivation for Developing a Parity Violation Experiment

When analyzing the experiments mentioned above, it is interesting to note that every single experiment was performed by graduate students or professional research scientists. In fact,

there are currently no experiments published for demonstrating parity violation in undergraduate laboratories. Many previous experiments involved difficult, time-consuming procedures or required equipment that is not readily available for undergraduate laboratories. Take Wu's experiment for example. The equipment needed for her experiment, such as the cryostat, would be difficult to obtain for an undergrad laboratory. Add to this the complicated nature of the experiment itself and it would be hard to replicate in a limited time with limited resources. An apparatus like Lundby's is a much more feasible option for undergraduate laboratories all-around; it requires fewer detectors, does not require the source to be polarized, and has no moving parts. The experiment at Houghton University transfers the idea of a more simplistic design from the Lundby et al. experiment to a new parity violation experiment that used more modern detectors and improved electronics. This experiment was developed with the constraints of the typical undergraduate laboratory in mind, as it is intended to be used and replicated. This experiment is intended to make phenomenon of parity violation, one of the most important discoveries of the 20th century, more widely available to undergraduate students. The experiment at Houghton University is not intended to be exclusive to Houghton physics students, but rather serve as an example for other undergraduate programs to follow in creating their own experiments.

1.5. Introduction of the Experiment at Houghton University

While there are no experiments exactly like the experiment at Houghton University, it is most closely related to the Lundby et al. experiment. Like the Lundby et al., Schopper et al., and the first Goldhaber et al. experiments, the experiment at Houghton will use the transmission method to look for parity violation in the weak nuclear force. The Houghton experiment will use ^{60}Co as the source for beta decay electrons and subsequent coincident circularly polarized gammas. The experiment will use ^{60}Co because of the way it decays into a stretched state, meaning the spins of all the particles must be in the same direction to conserve angular momentum.

As shown in Figure 7, the source will be centered on top of an electromagnet, whose electron magnetic dipoles can be oriented upwards or downwards based on the direction of current within the magnet's coils. A silicon detector will be placed directly above to count the

electrons emitted vertically from the source, while an NaI detector will be placed directly below the source on the opposite side of the electromagnet's core to count the gamma rays in coincidence after they pass through the electromagnet. This will be to confirm that both detectors are indeed triggering on the same event. Coincidence counting rates will be measured for beta events and gamma rays with each magnetic dipole orientation (up or down). The number of gamma rays that pass through the electromagnet with each magnetic dipole orientation will be counted. Just as in the previous experiments, the electron spins for each magnetic dipole orientation will scatter right and left circularly polarized gamma rays differently. If parity is violated, there should be an asymmetry between the number of gamma rays transmitted through the electromagnet for the two magnetic dipole measurement orientations.

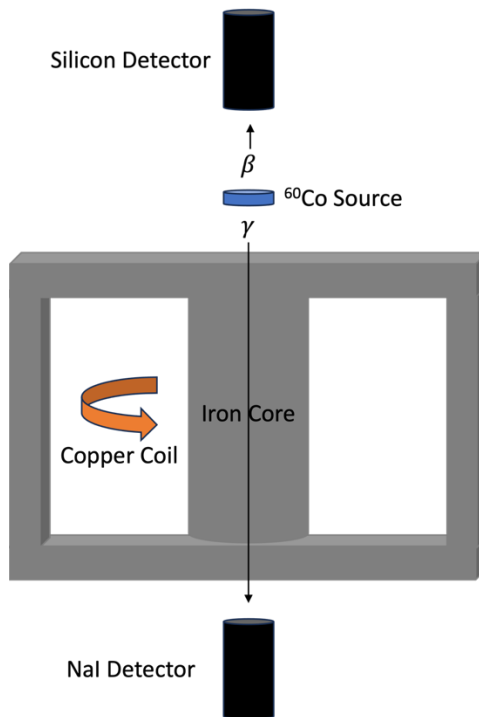


Figure 7. Simplified diagram of the Houghton University experiment. The ^{60}Co source will be centered on top of the magnet core. Beta events will be measured by the silicon detector while gamma particles will be measured by the NaI detector after passing through the electromagnet core. Gamma events will be verified by their coincidence with beta events. The copper coils will be responsible for aligning the magnetic dipole moments of the electrons in the magnet core. The direction can be reversed by reversing the current through the coil.

The key to this experiment will be achieving sufficient detector energy resolution to accurately measure the number of gamma rays, proper magnet saturation to ensure enough of the magnetic dipoles will be aligned, and proper magnet thickness to provide sufficient event numbers while still effectively scattering enough gamma particles so show a measurable asymmetry between the two measurements. Ultimately, a statistically significant difference in coincidence rates through each magnetic dipole orientation would indicate that the gamma rays are biased to one helicity over the other. If this is the case, the same experiment performed in a mirrored universe would conclude that the gamma rays are bias to the opposite helicity, allowing the experimenter to tell if they were in the original or mirrored system. This would be evidence of parity violation.

Chapter 2

THEORY OF PARITY VIOLATION

2.1. Theory Overview

The Houghton University parity violation experiment is dependent on two particular elements in order to properly test parity violation in the weak nuclear force. The first element is utilizing a source that undergoes a parity-violating weak nuclear decay. Section 2.2 will explain why and how ^{60}Co satisfies this requirement. The second critical element is the ability to measure the asymmetry, which is achieved by transmission through an electromagnet, as shown in Figure 7. The magnet must be the proper thickness to show a statistically significant asymmetry measurement; these predictions will be detailed in Section 2.3.

2.2. Beta Decay of ^{60}Co

To understand why the gamma rays emitted in coincidence with beta events in ^{60}Co have a left or right-handed circular polarization, the unique characteristics of beta decay in ^{60}Co must be closely examined. A right-handed gamma ray has z-component of spin and momentum in the same direction, while a left-handed gamma ray has z-component of spin and momentum in opposite directions. Figure 8 shows the decay scheme of ^{60}Co , which starts in the spin 5 ground state. What is important to note is how angular momentum is conserved as the ^{60}Co nucleus decays to ^{60}Ni . The “spins” shown in Figure 8 refer to the quantized levels of the z-component of the angular momentum of the nucleus. The ground state of ^{60}Co has spin 5, which beta decays 99.88% of the time to the stretched state of ^{60}Ni , spin 4. A 1.1732-MeV gamma ray and a 1.3325-MeV gamma ray are subsequently released, each with spin 2. The ground state of ^{60}Ni is left with spin 0. This means that all spins must be in the same direction as the ^{60}Co spin to conserve angular momentum. Figure 9 shows how the z-component of is related to the distribution of angular momentum. Since J_z is quantized, J can point anywhere along the cone shown in Figure 9. $J_z = m\hbar$, where $m = -j, -j + 1 \dots j$, and j has allowed values $j = 0, 1, 2 \dots$.

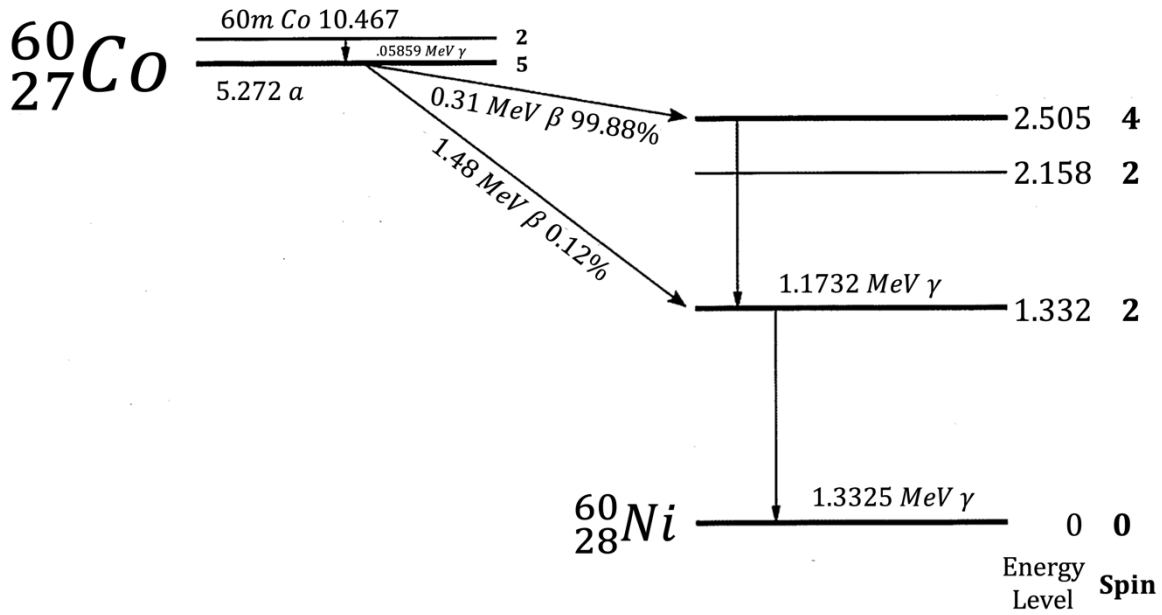


Figure 8. Energy level diagram of ^{60}Co . The spin-5 ground state of ^{60}Co decays 99.88% of the time by emitting a 0.31 MeV-end point beta particle to the spin-4 excited state of ^{60}Ni at 2.505 MeV. The nucleus then releases two gamma rays, each with spin 2. Thus, since ^{60}Co has spin 5 and ^{60}Ni has spin 0, and the sum of the spins of each emitted particle must be 5, meaning they all must be in the same direction as the ^{60}Co spin. Data obtained from the IAEA Nuclear Data Services website [13].

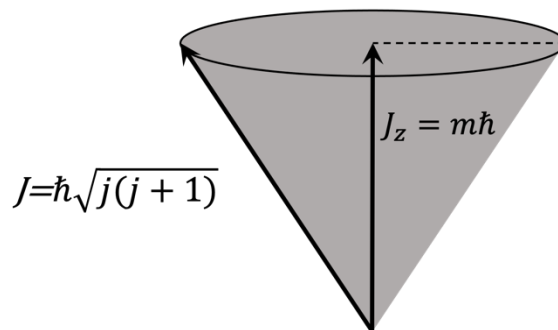


Figure 9. Quantization of the z-component of angular momentum. The magnitude of angular momentum $J = |J|$, and J_z is the magnitude of the component of angular momentum J in the z-direction. Since J_z is quantized, J can point anywhere along the cone. The angular momentum quantum number j has allowed values $j = 0, 1, 2 \dots$ for orbital angular momentum, and for spins $j = 0, \frac{1}{2}, 1, \frac{3}{2}, \dots$. The quantum number m is $m = -j, -j + 1, \dots, j$.

The conservation of the z-component of angular momentum, J_z , is shown in Figure 10. The first decay is a beta decay in which the spin 5 ^{60}Co emits an electron and neutrino, each particle with respective spin 1/2. The remaining excited ^{60}Ni nucleus has spin 4. The only

way to conserve angular momentum is if the z-components of all spins point in the same direction – this is called the stretched state. Two gamma rays are then emitted from the spin 4 ^{60}Ni nucleus, each with spin 2. This leaves the nucleus in the ground state of ^{60}Ni . To conserve angular momentum, the z-component of both gamma rays must point in the same direction as the original ^{60}Co nucleus.

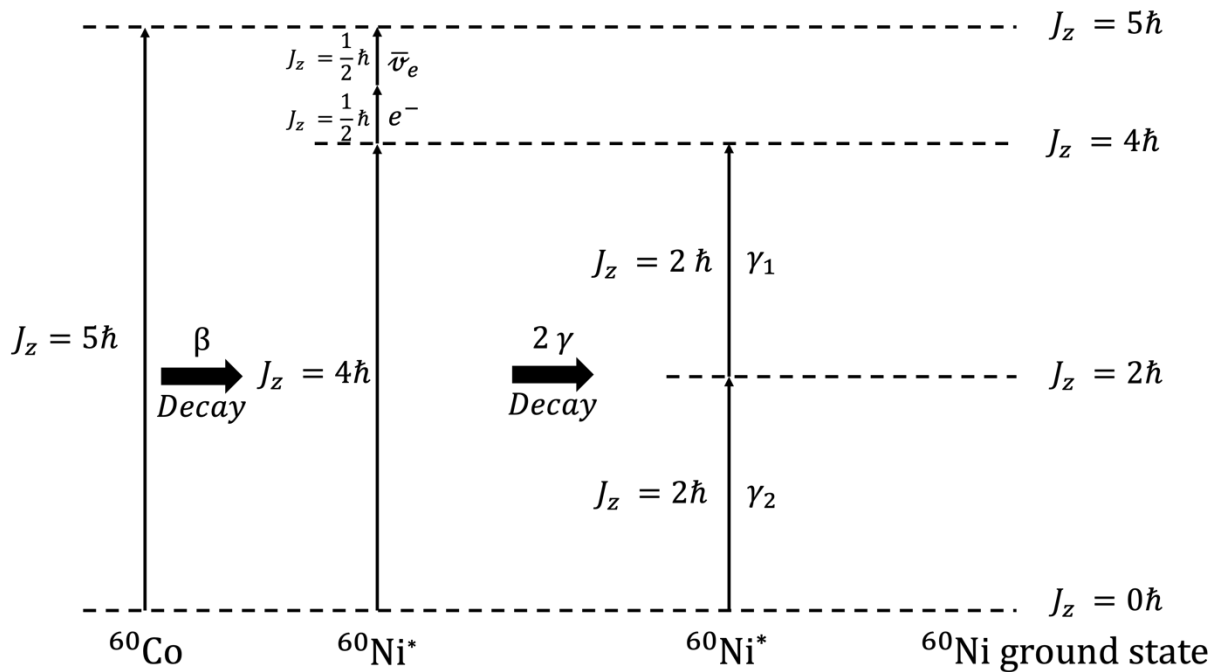


Figure 10. Conservation of the z-component of angular momentum. The first decay is a beta decay as ^{60}Co transitions to the first excited state $^{60}\text{Ni}^*$. The beta decay consists of an electron and antineutrino, each with $J_z = \frac{1}{2}\hbar$. This leaves the remaining excited ^{60}Ni nucleus $J_z = 4\hbar$. Two gamma particles then decay in sequence; each gamma has $J_z = 2\hbar$. This leaves the nucleus in the ground state of ^{60}Ni .

While Figure 10 indicates how the z-component of angular momentum is conserved throughout the decay process, it does not account for the direction of the decay particles' momenta as they are released from the ^{60}Co nucleus. There are three rules that must be obeyed to conserve momentum when specifying the directions of the momenta of these particles relative to the spin of the parent nucleus. (1) The antineutrino always has momentum and spin in the same direction. (2) The spin of a circularly polarized gamma

ray must be either parallel or antiparallel to its momentum. (3) Finally, the spin and momentum of a beta particle can be in any direction relative to each other.

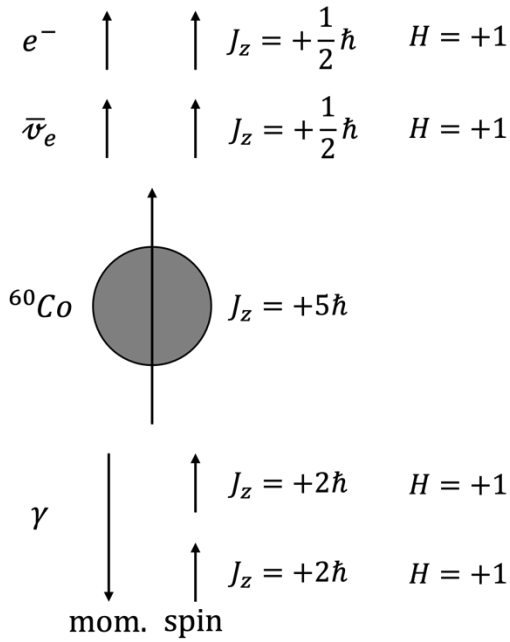
When talking about the spin and momenta of particles, it is important to understand how these two elements result in the helicity of the particle. Helicity is the projection of the spin of a particle onto the direction of its momentum, given by the equation:

$$H = \frac{\vec{s} \cdot \vec{p}}{|\vec{s} \cdot \vec{p}|} \quad (1)$$

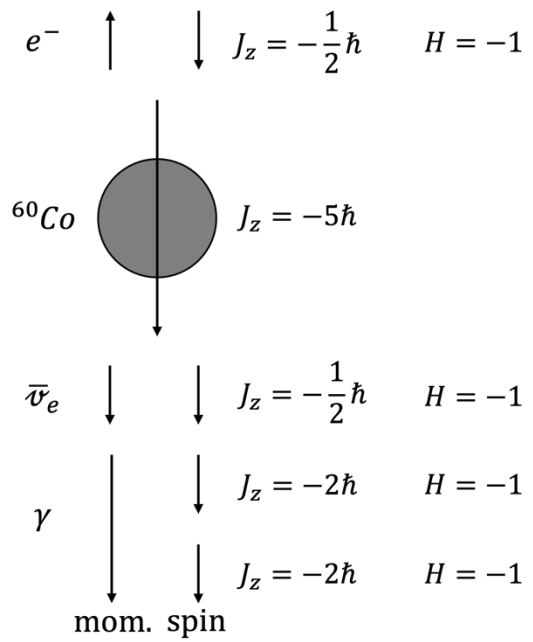
Consider Figure 11, which depicts the direction of momentum and spin for each particle in a decay where the beta particle and gamma ray are travelling in opposite directions. This is forced by taking beta and gamma coincidence pulses. To conserve angular momentum, all spins must point in the same direction, as seen in the stretched state of ^{60}Ni in Figure 10. While this does not affect the momentum of the gamma or beta particles, it does affect the momentum of the antineutrino, whose spin and momentum must be in the same direction. Mirroring the ^{60}Co nucleus with an upwards spin (lower left of Figure 12) showed a ^{60}Co nucleus with a downward spin, as well as reversed all the other particles' spins (lower right of Figure 12). The mirrored system was not possible, as it still showed the momentum and spin of the antineutrino in opposite directions. Note Figure 12, which shows the impossible results if the two viable decay options were to be mirrored. When either option was mirrored, the antineutrino violated parity symmetry, and since the antineutrino violated parity symmetry, the system violated parity symmetry.

The antineutrino is difficult to detect, and thus will be ignored as a way to distinguish between the two states. This leaves the circularly polarized gamma rays and the beta particles shown in Figure 13 as the viable option for measuring parity asymmetry. For parity to be violated, one of the two states on the left side of Figure 12 must be shown to be more likely than the other. Measuring the beta particles directly requires source polarization as in Wu's experiment, which is difficult to achieve in most undergraduate laboratories. This leaves the circular polarization of the gamma rays opposite the beta as the most viable option for testing parity asymmetry.

β in direction of ^{60}Co spin



β in opposite direction of ^{60}Co spin



Note that all spins must be in same direction as ^{60}Co spin

Figure 11. Two possible particle spins and directions of momenta. These configurations are based on parent nucleus spin for beta and gammas emitted in opposite directions. To conserve angular momentum, the spins of all the particles must be in the same direction for each respective system. Since the spin and momentum of an antineutrino must be in the same direction, the direction of the antineutrino's momentum must switch when the direction of the ^{60}Co nucleus spin switches directions. Thus, these are the only two decay options that follow all the rules. Also note that the helicity of the gamma particles are different depending on the spin of the parent nucleus, which results in two different circular polarization states of the gamma rays.

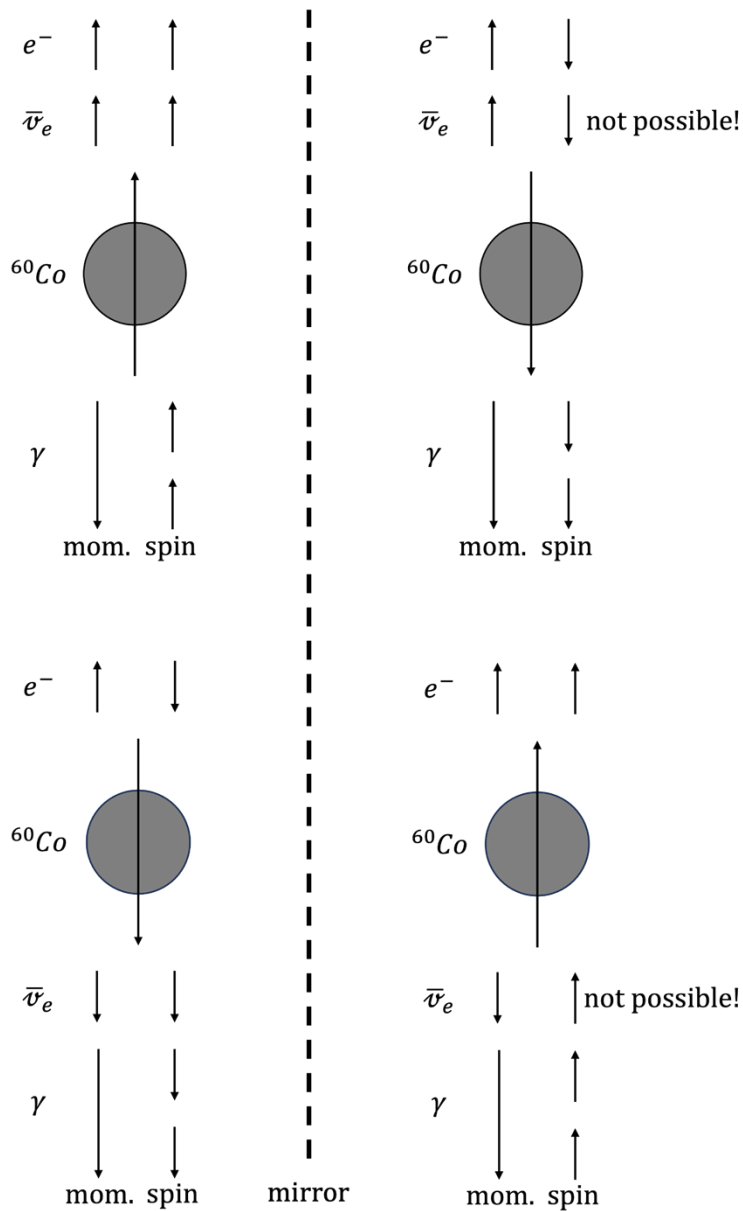


Figure 12. Mirrored ^{60}Co decays showing impossible “configurations.” Upper right nucleus and lower left nucleus showed the two possible configurations shown in Figure 11. Both configurations were mirrored, and due to the inversion of the spin direction under a mirror transformation, the mirrored decays both showed antineutrinos with spin and momentum in opposite directions. Whether the spins are aligned up or down, neither mirrored configuration is possible since the spin and momentum of the antineutrino must be in the same direction. This means the antineutrino violates parity symmetry, and thus the beta decay of ^{60}Co violates parity symmetry. If parity was not violated, the mirror configurations would be just as likely as the original configurations.

These two circular polarizations have different Compton scattering cross sections when scattering through an electromagnet with an oriented magnetic field, meaning different numbers of gamma rays will be transmitted through the electromagnet when the magnetic field is oriented parallel versus antiparallel to the spin of the gamma rays. If there are equal numbers of each circular gamma polarization attempting to pass through the magnet, the coincidence count number will be the same regardless of magnetic field direction. If there is an asymmetry in the number of right and left circular gamma polarizations, there will be an asymmetry in the coincidence count number with each magnetic field direction. This asymmetry can be quantified using the equation

$$E = \frac{N_+ - N_-}{\frac{1}{2}(N_+ + N_-)} \quad (2)$$

where E is the asymmetry, N_+ is the number of coincidence events with a parallel field, and N_- is the number of coincidence events with an antiparallel field. If there is no asymmetry, N_+ and N_- will be equal and $E = 0$. This idea will be explored more in the next section.

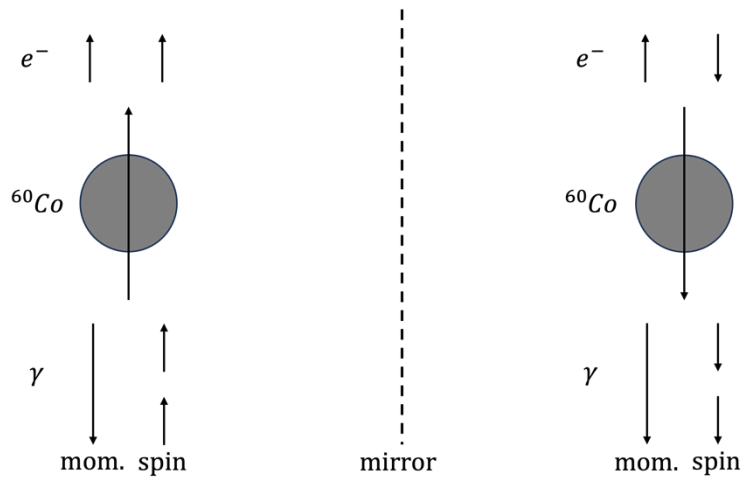


Figure 13. The two decay configurations without antineutrinos. Since antineutrinos cannot be measured effectively, the experiment only measures beta particles and gamma rays. These two configurations are the only two possible and are “mirror images” of each other. The gamma ray on the left will have a left circular polarization, and the gamma ray on the right will have a right circular polarization. These two circular polarizations will result in different Compton scattering cross sections, and thus can be differentiated between when transmitted through an electromagnet. There must be a measurable difference between the two sides for parity violation to be shown.

2.3. Gamma Transmission Asymmetry Calculation

The idea of an asymmetry in gamma ray transmission rates through an electromagnet based on the circular polarization of the gamma rays and the magnetic dipole orientation of the electromagnet are a result of Compton scattering, which is the interaction between the gamma rays and the electrons surrounding the nuclei that make up the core of the electromagnet. The following derivation of the expected transmission rates for the two different gamma rays as they are Compton scattered through the electromagnet as seen in Figure 14 roughly follows Schopper's derivation in Ref. [11].

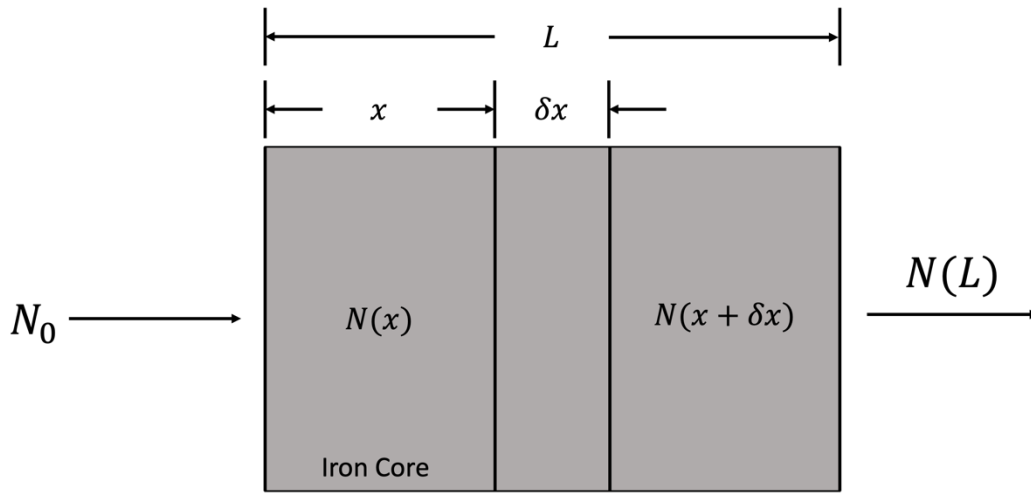


Figure 14. Gamma transmission through polarized magnet core. Gamma transmission depends on the thickness of the iron core. Consider a slice of the core with thickness δx , located a distance x into the core of total length L . The number of gamma rays passing through the surface at x is given by $N(x)$, and the number of gamma rays passing through the surface at $x + \delta x$ is given by $N(x + \delta x)$, thus the total number of gamma rays scattered by a thickness δx of the core is given by $N_s = N(x) - N(x + \delta x)$.

Now we consider a gamma ray penetrating a thickness of iron. From Figure 14, we see that the number of gamma rays scattered, N_s , by a slice of thickness δx located at distance x in the core is given by

$$N_s = N(x) - N(x + \delta x), \quad (3)$$

where $N(x)$ is the number of gamma rays that penetrate to distance x . N_s , however, is proportional to the number density of electrons (N'_t), the number of gammas crossing into the slice at x ($N(x)$), and the thickness of the slice. The constant of proportionality is the

cross section σ which has units of 1/area. This means that $N_s = \sigma N_t' N_{inc} \delta x$. The density of electrons is given by $N_t' = ZN_t$ where Z is the number of electrons/atom and N_t is the density of iron atoms, thus,

$$N(x) - N(x + \delta x) = \sigma Z N_t N(x) \delta x. \quad (4)$$

This can be solved for $N(x)$, or the number of gamma rays transmitted through a thickness of iron x . Take the limit as $\delta x \rightarrow 0$, so that a derivative is obtained:

$$\sigma Z N_t N(x) = \lim_{x \rightarrow 0} \frac{N(x - \delta x) - N(x)}{\delta x} = \frac{dN}{dx}. \quad (5)$$

This can be solved using a single integral, which yields

$$N(x) = k e^{-\sigma Z N_t x}. \quad (6)$$

When $x = 0$ the number of gamma rays is N_0 , so $k = N_0$. Thus, the transmission of gamma rays through the iron is given by

$$N(x) = N_0 e^{-\sigma Z N_t x}. \quad (7)$$

The Compton scattering cross section σ can be broken into two parts [11], one of which, σ_c , depends on the orientation of the gamma and electron spins. Thus,

$$\sigma = \sigma_0 + f P_c \sigma_c, \quad (8)$$

where

$$\sigma_c^\pm = \pm 2\pi r_0^2 \left(\frac{1 + 4k_0 + 5k_0^2}{k_0(1 + 2k_0)^2} - \frac{1 + k_0}{2k_0^2} \ln(1 + 2k_0) \right); \quad (9)$$

here + signifies the electron spin (of the iron nuclei) is parallel to the gamma ray spin, - signifies the electron spin is antiparallel to the gamma ray spin, $r_0 = ke^2/mc^2 = 2.82$ fm (the classical electron radius), $k_0 = h/\lambda = E/e$, or the initial gamma ray momentum, f is the fraction of oriented electrons in the electromagnet, $Zf = \nu$ is the number of oriented electrons per atom in the electromagnet, and P_c is the degree of circular polarization of the gamma rays, where 1 means complete polarization. Clearly, we can define:

$$\sigma_c \equiv \sigma_c^+ = -\sigma_c^-. \quad (10)$$

We can therefore find the gamma transmission rates when the electron spins are aligned parallel, N_+ , and antiparallel, N_- from Eq. 7 and 8:

$$N_+ = N_0(e^{-\sigma_o Z N_t x} e^{-f P_c \sigma_c Z N_t x}) \quad (11)$$

and

$$N_- = N_0(e^{-\sigma_o Z N_t x} e^{f P_c \sigma_c Z N_t x}). \quad (12)$$

Thus, the asymmetry, E , between the two counting rates for 100% right-handed versus 100% left-handed gamma polarization is given by

$$E = \frac{N_+ - N_-}{\frac{1}{2}(N_+ + N_-)}. \quad (13)$$

Substitute in for N_+ and N_- , such that

$$E = \frac{N_0(e^{-\sigma Z N_t x} e^{-f P_c \sigma_c Z N_t x}) - N_0(e^{-\sigma Z N_t x} e^{f P_c \sigma_c Z N_t x})}{\frac{1}{2}(N_0(e^{-\sigma Z N_t x} e^{-f P_c \sigma_c Z N_t x}) + N_0(e^{-\sigma Z N_t x} e^{f P_c \sigma_c Z N_t x}))}, \quad (14)$$

which can be simplified as

$$E = 2 \tanh(-f Z N_t \sigma_c P_c x). \quad (15)$$

Remember that $v \equiv Zf$; simplifying the equation in this way results in

$$E = 2 \tanh(-N_t v \sigma_c P_c x), \quad (16)$$

which agrees with the result given by Schopper in Ref. [11]. These predictions show a difference between the measured gamma transmission rates when the magnetic dipoles are polarized parallel versus antiparallel. If the gammas from the source have equal numbers of right-handed and left-handed gamma rays, there will be no total asymmetry, $E = 0$. If, however, $E \neq 0$ is measured, it will mean there are more right-handed than left-handed gamma rays (or vice versa), indicating parity symmetry has been violated.

The predicted asymmetry as a function of magnet core thickness is shown in Figure 15, while the number of predicted transmitted gamma rays as a function of thickness is shown in Figure 16. Notice that as the core thickness increases, the uncertainty bars increase faster. This is because transmission numbers decrease exponentially as thickness is increased. A

thinner magnet core shows a small asymmetry, E , with small uncertainty, while a thicker magnet core shows a large asymmetry with large uncertainty due to much lower transmission rates.

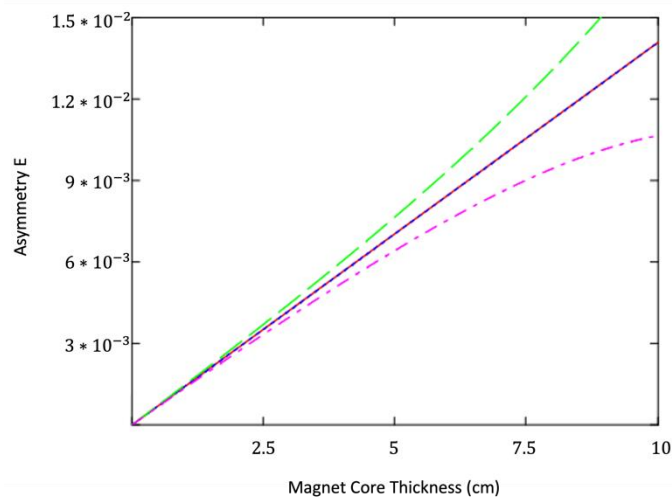


Figure 15. Plot of predicted gamma asymmetry as a function of core thickness. In this instance, the thickness of the magnets core is in centimeters. The theory prediction shows a linear increase in the amount of measurable gamma asymmetry as the core thickness increases. The red line is the direct asymmetry, while the blue dotted line is the approximate asymmetry. The top green and bottom purple curves are the error bars, which increase faster than the asymmetry.

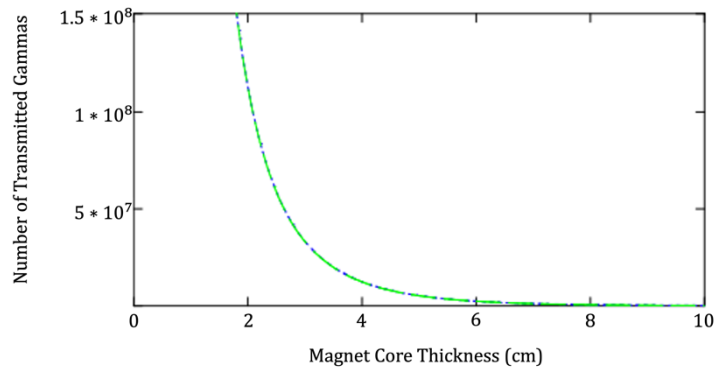


Figure 16. Plot of predicted gamma transmission versus core thickness. The x-axis is thickness of the electromagnet core in cm; the blue line is the number of parallel spin gamma rays transmitted, while the green line is the number of antiparallel spin gamma rays transmitted. The plot predicts that as the thickness of the core increases, the number of gamma rays transmitted through the electromagnet will decrease exponentially. This is the reason for the exponentially increasing error bars in the plot in Figure 15.

The best value for core thickness can be found using the ratio of uncertainty to asymmetry, or, relative uncertainty, which is given by

$$\frac{\Delta E}{E} = \frac{\text{uncertainty}}{\text{asymmetry}} \tag{18}$$

The best magnet thickness will be where the relative uncertainty is lowest, thus we can plot relative uncertainty versus magnet thickness to find the thickness with the minimum value of relative uncertainty. Figure 17 shows a minimum between 4-5 cm.

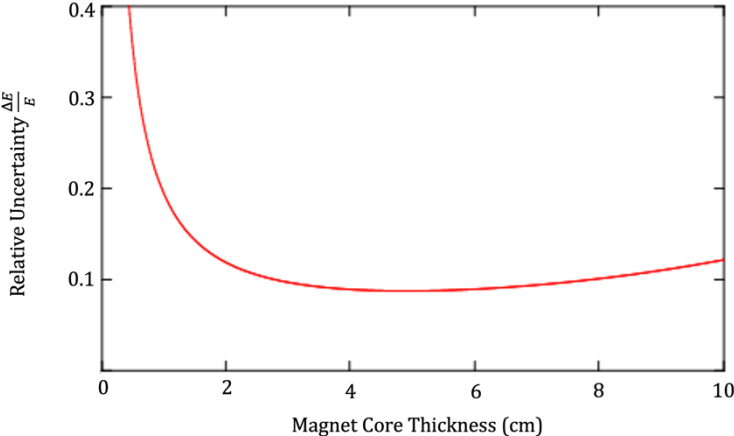


Figure 17. Plot of predicted relative uncertainty versus core thickness. The red line on the plot shows a minimum relative uncertainty between 4 and 5 cm, which would be the ideal core thickness.

Chapter 3

EXPERIMENT

3.1. *Experimental Overview*

The design of the transmission experiment to test parity violation is shown in Figure 18. The experiment starts with a $1 \mu\text{Ci } ^{60}\text{Co}$ source, which undergoes beta decay and emits electrons and circularly polarized gamma rays opposite one another as described in Section 2.2. The electrons are detected by a silicon detector, while the gamma rays are transmitted through the electromagnet core – the gamma rays that pass through without scattering are measured by a NaI detector on the other side of the electromagnet. The source, magnet, and both detectors are aligned coaxially. Pulses from both detectors are then sent to their respective pre-amplifiers, where each pulse is inverted, integrated, and amplified. These modified pulses are then sent to their respective timing filter amplifiers, where the pulse shapes are differentiated, shaped, and amplified. Coincidence pulse timing is adjusted to account for the minute differences in travel time through the different parts of the circuit. Both pulses arrive at the FemtoDAQ, which digitizes the pulse height for each pulse in coincidence and records this information along with a time stamp.

3.2. *Electromagnet*

The purpose of the electromagnet is to “filter” gamma rays by Compton scattering the circularly polarized gamma rays through parallel and antiparallel magnetic field orientations. The two different circular polarizations scatter differently from the polarized electrons in each orientation, giving non-zero asymmetry unless there are equal numbers of right-handed and left-handed gamma rays coming from the source. Design of the electromagnet began with the calculation shown in Appendix A to determine the magnet parameters needed to achieve the desired magnetic field and resulting electron polarization saturation necessary to minimize the asymmetry uncertainty, while still maintaining a viable counting rate. The calculations in Section 2.3 were helpful for determining the proper dimensions of the electromagnet yoke, as they allow for the calculation of both asymmetry and transmission rate as a function of thickness.

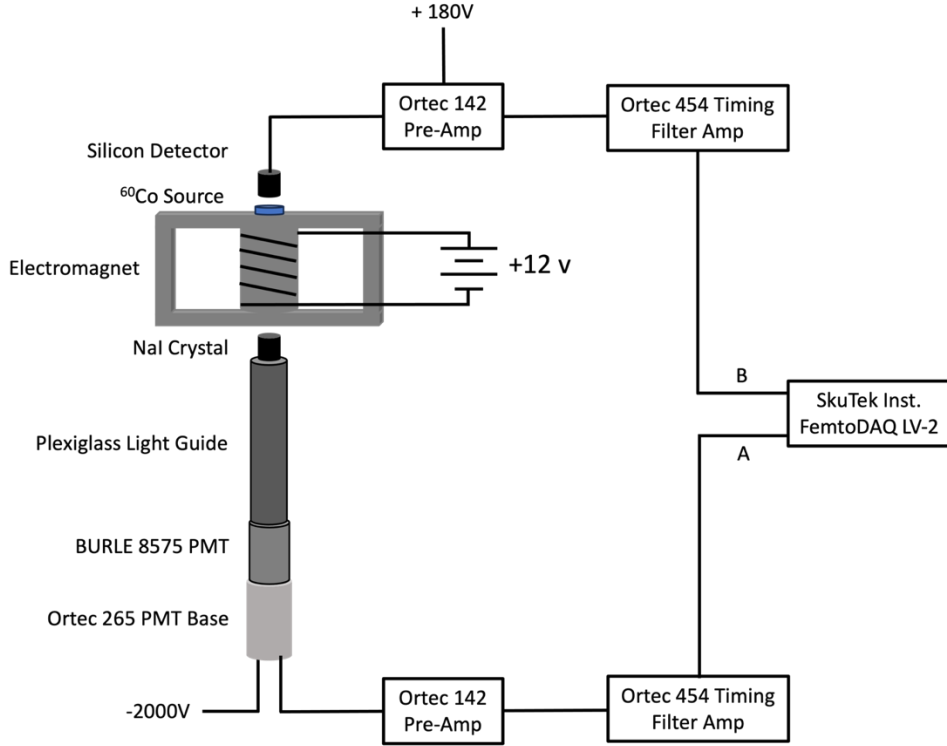


Figure 18. Block diagram of Houghton transmission experiment. Betas and gamma rays were emitted from the source. Gamma rays were detected by the NaI detector after passing through the electromagnet, and coincidence betas were detected by the silicon detector. The betas and gamma rays deposit their energy in the detector, which sends that energy to the rest of the circuit in the form of an electrical pulse. These pulses are shaped, timed, and prepared for the digitizer. After the digitizer verified the pulses were within an acceptable timing range to be considered “coincidence,” it recorded the pulse heights and their time stamp.

The SMath calculations in Appendix A use Ampere’s law as shown in Ref. [15] to estimate the field strength of the electromagnet (H) at the point where the steel is adequately saturated. The calculations start with Ampere’s law,

$$\oint \mathbf{H} \cdot d\mathbf{l} = NI, \quad (19)$$

where N is the number of turns, I is the current through the coil, and $d\mathbf{l}$ is the length around a path. By applying Ampere’s circuital law and assuming no flux leakage,

$$NI = H_c L_c + H_y L_y. \quad (20)$$

H_c is the magnetic field intensity in the core, and L_c is the path length through the core. H_y and L_y are the same respectively, but for the yoke. In a normal electromagnet, there is an air

gap that must be accounted for, however since the sole purpose of this magnet is to saturate the steel, an air gap is not necessary. Applying the fact that $\nabla \cdot \mathbf{B} = 0$,

$$B_c A_c = B_y A_y, \quad (21)$$

where A_c and A_y are the cross sections of the core and the yoke, respectively. Combining these two equations results in

$$B = \frac{NI\mu}{A \left[\frac{L_c}{A_c} + \frac{L_y}{A_y} \right]}, \quad (23)$$

where μ is the core and yoke permeability. The simulated electromagnet was assumed to be made of steel with relative permeability of 100, and the overall dimensions were 15.24 cm (6 in) in length, by 5.635 cm (2 in) in total height, by 8.89 cm (3.5 in) in depth. The core was 3.81 cm (1.5 in) in diameter by 3.81 cm (1.5 in) in height, with a surrounding yoke made of 0.635 cm (0.25 in) steel plates. The wire required for 1500 turns amounted to a total resistivity of 12.272 ohms, and 1 amp of current passed through the coil amounts to a simulated magnetic field of 0.7801 Tesla.

Another way that the magnet was modeled is shown in Figure 19. Created using Radia [14] in Mathematica, the plot depicts the vector model of the field looking side-on at the long edge of the magnet. From the simulation it was determined that these parameters created a field sufficient to saturate the core. This conclusion is based on how parallel (to the z-axis) the magnetic field lines stay throughout the core; the center of mass of the core is at (0,0), and the core dimensions are 38.1 mm by 38.1 mm.

After determining that these electromagnet parameters would be sufficient to create the desired asymmetry, the electromagnet core and yoke were designed to these parameters using AutoCAD Inventor as shown in Figure 20. The 1018 low carbon cold rolled steel with relative permeability of about 500 (significantly more than the simulation) was then milled to the correct dimensions using an upright mill, starting by squaring one side with an end mill bit, and then squaring and dimensioning each other sides based off the first squared side.

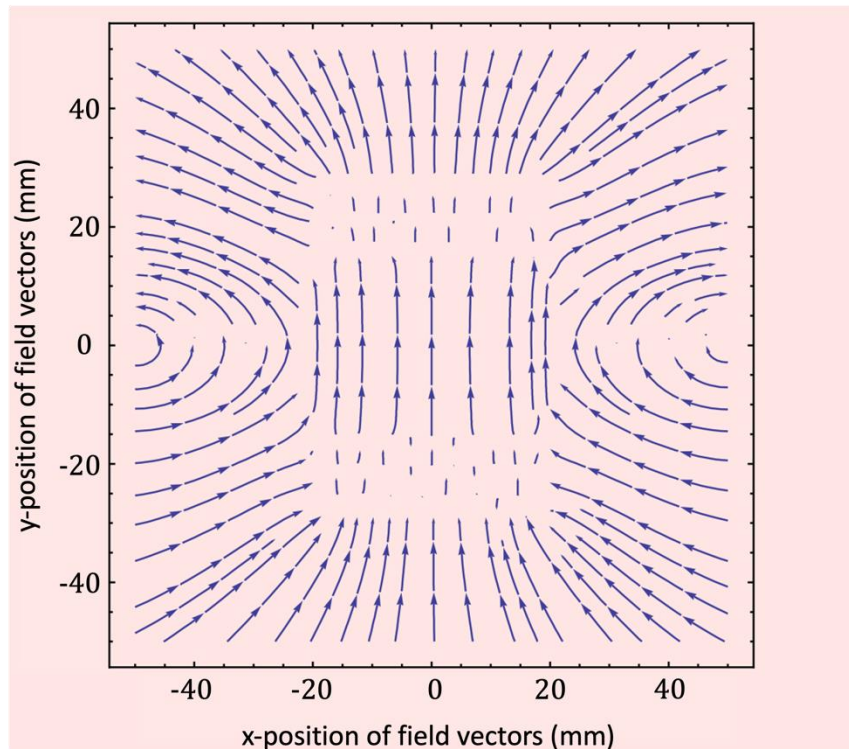


Figure 19. Vector field representation of the simulation of the magnet field. The field model shows the magnetic field almost completely vertical throughout the core, which would be roughly -20 mm– 20 mm on the x-axis, and -20 mm – 20 mm on the z-axis. The core dimensions are 38.1 mm by 38.1mm, and (0, 0) corresponds to the center of mass of the core. Complete core electron saturation would result in a magnetic field that is completely parallel to the z-axis throughout the entirety of the core. Higher core electron polarization results in a lower uncertainty in asymmetry measurements. Based on this model, the field should cause adequate core electron polarization saturation.

The yoke consisted of five different pieces total, two 8.89 cm × 3.81 cm × 0.635 cm (3.5 in × 1.5 in × 0.25 in), two 8.89 cm × 15.24 cm × 0.635 in (3.5 in × 6 in × 0.25 in), and the 3.81 cm in diameter core, which was turned on the lathe to a length of 3.81 cm. The four sides were secured together in a rectangular formation, with the two small plates inside the two larger plates to create an overall yoke height of 5.08 cm (2 in) as shown in Figure 21. The plates were attached via 8 #6 by 1.27 cm (0.5 in) steel flathead screws, one in each corner; clearance holes were drilled through the corners of each of the large plates, and holes were drilled and tapped in the corners of each 8.89 cm by 0.635 cm side of the smaller plates for the eight screws, one in each corner. The core was friction fit in the center of the yoke, and the screws were tightened on the assembly such that the core was in solid contact with each

plate above and below, as well as solid contact between the edges of the large and small rectangular plates. The steel assembly was painted with a layer of Seymour Farm and Industry protective spray paint once assembled to prevent rust or corrosion, while maintaining the metal-on-metal connections between the different components of the magnet yoke.

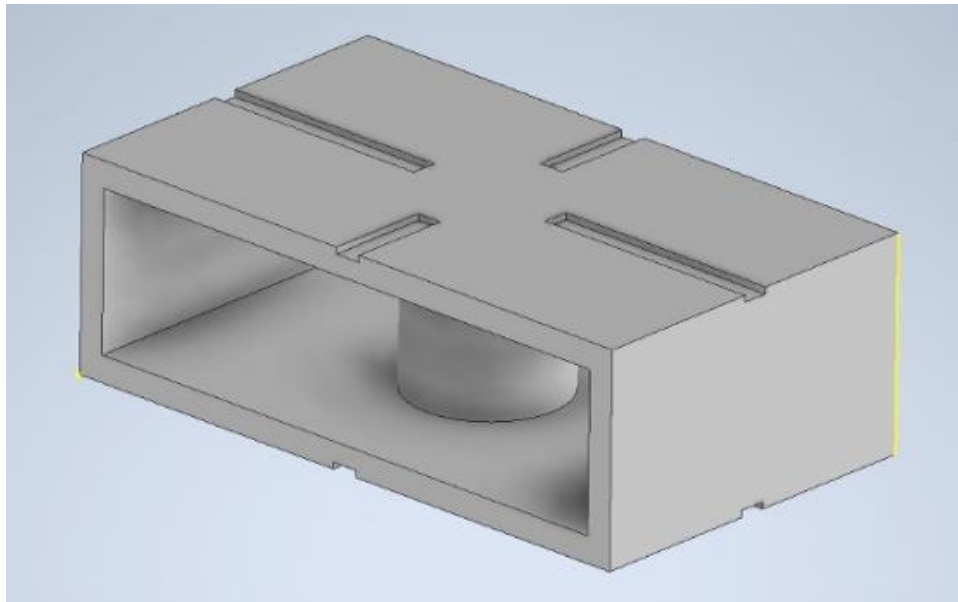


Figure 20. CAD drawing of electromagnet yoke. The dimensions of this model were matched to the dimensions of the yoke in the simulated electromagnet. The yoke was made of 5 total pieces of 1018 low carbon cold rolled steel; two 8.89 cm × 3.81 cm × 0.635 cm (3.5 in × 1.5 in × 0.25 in) plates, two 8.89 cm × 15.24 cm × 0.635 in (3.5 in × 6 in × 0.25 in) plates, and the 3.81 cm diameter core, which was turned on the lathe to a length of 3.81 cm. The two smaller plates were secured in between the two larger plates such that the final outer dimensions of the yoke were 15.24 cm by 8.89 cm × 5.08 cm. The grooves seen in the yoke were initially meant to help align the detectors, however 3D printed parts were used instead because of the ease of manufacturing, as seen in Figure 21.

Next was the task of wrapping the coils around the core. A bobbin was designed as shown in Figure 22 and 3D printed to slide over the core and retain the coils; the bobbin was also designed to keep the core aligned coaxially with the center of the top and bottom large plates. According to the simulation, 1500 total turns of copper magnet wire was necessary for optimal saturation of the steel. The 20 AWG insulated copper magnet wire was wound by

hand turning the bobbin and feeding the wire in even layers back and forth across the bobbin until 1500 turns were completed.

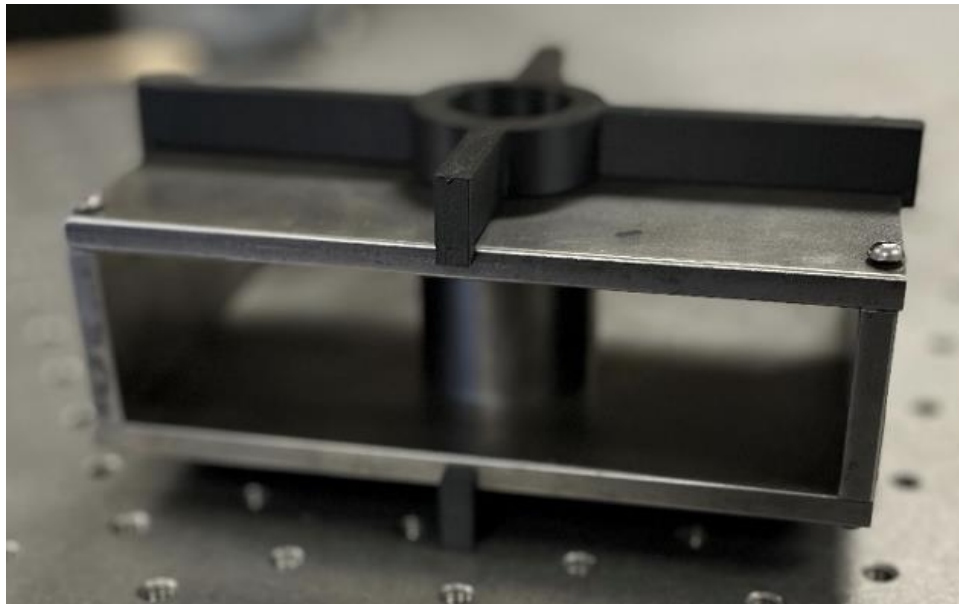


Figure 21. Picture of completed (but not yet painted) electromagnet yoke. Notice that the two smaller plates were secured in between the two larger plates using a screw on each corner. The core was friction fit in between the top and bottom plates; tightening the screws in each corner secured the core in place. The 3D printed parts on top and bottom of the yoke were designed to properly align the silicon and NaI detectors.

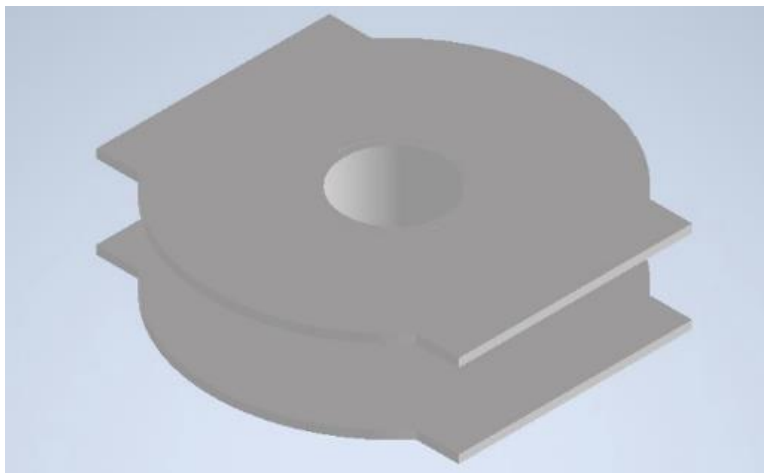


Figure 22. AutoCAD design of bobbin which housed the magnet's coil. The bobbin matched the interior dimensions of the yoke, properly aligning the core which was fit through the center of the bobbin.

The fixture in Figure 23 was created to allow the bobbin to be spun freely, while the spool of wire was set to allow the wire to be pulled directly from the spool and wrapped onto the bobbin. The spool was tensioned so that the wire would wrap snugly onto the bobbin. This process was done completely by hand and was extremely time consuming, with the main problems arising when the wire became un-tensioned, causing the coil to unwind – a better process for this task could be developed in the future. Another problem was the bobbin strength, which warped and broke under the pressure of the coil. A strong enough bobbin was eventually produced by increasing the fill of the 3D print; a better bobbin material could be utilized in the future. After the coil was completely wrapped on the bobbin, the assembly was then inserted onto the core, and core, bobbin, and wire were clamped into place with the other outer components of the electromagnet as described above. A large enough voltage bias would be applied across the coil to induce 1 A of current (roughly 12 V considering the resistance of the coil), which should be sufficient to create the desired magnetic field strength considering the significantly higher relative permeability of the steel used, however the magnetic field has not yet been measured. The completed assembly is shown in Figure 24.

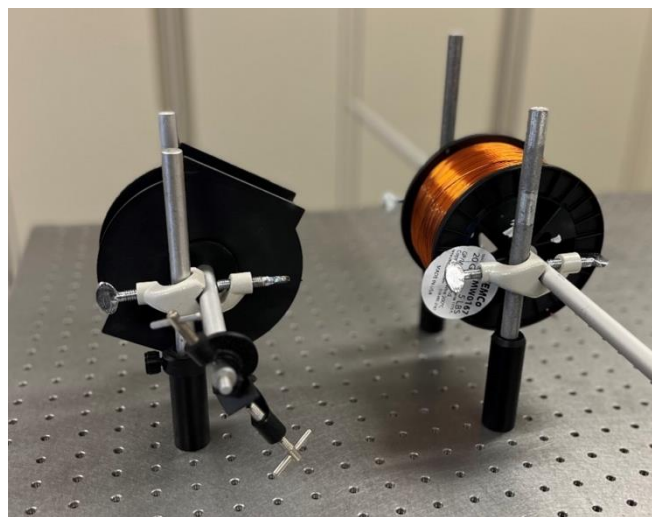


Figure 23. Apparatus for winding coil onto bobbin. The bobbin on the left could be spun freely, while the spool of wire on the right was adjusted to keep tension on the wire as it was being wrapped onto the bobbin. If a pause was taken in wrapping the bobbin, both bobbin and spool could be locked with the wire under tension to prevent the coil from unraveling. There were 1500 turns of wire added to the bobbin to align with the simulation. Winding the bobbin by hand in this way was an extremely time-consuming process.

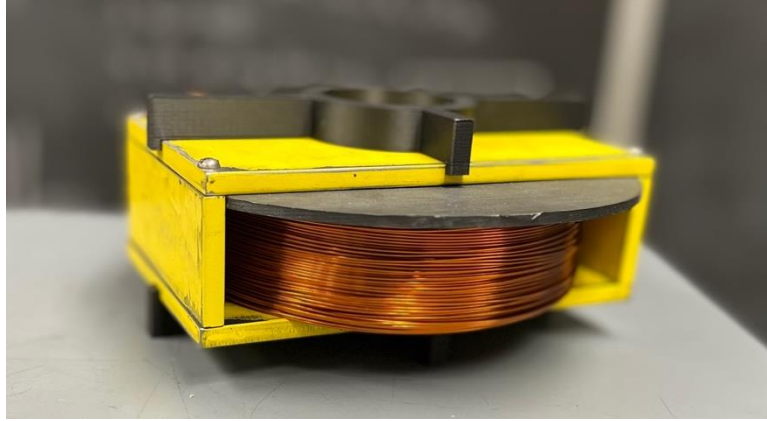


Figure 24. Completed electromagnet assembly. The coil and bobbin were inserted over the core and aligned in the yoke according to the bobbin. The screws on each corner were then tightened, securing the core in the yoke. Notice the yoke is painted with Seymore Farm and Industry protective spray paint to prevent rust.

3.3. Detectors

3.3.1. NaI Crystal Detector, Light Guide, PMT, and Base

The NaI crystal detector was responsible for counting the gamma rays that passed through the electromagnet without scattering. It utilized a hermetically sealed 3.81 cm diameter \times 3.81 tall (1.5 in \times 1.5 in) GammaSpectacular XL-NAI-1515 Sodium Iodide Crystal (NaI) to detect the gamma rays that pass through the electromagnet – the NaI crystal must be sealed, otherwise it will absorb water (from the air) and deteriorate over time. When a gamma ray strikes the NaI crystal, the crystal absorbs the energy from the gamma ray and emits a light pulse, which is transmitted to a BURLE 8575 photomultiplier tube (PMT) via a 5.08 cm (2 in) in diameter by 76.2 cm long (30 in) extruded acrylic light guide. The purpose of this light guide is to remove the PMT from the magnetic field of the electromagnet to ensure proper function. The PMT creates a cascade of electrons from the light pulse, and an Ortec 265 base attached to the PMT (operated at a bias voltage of -2000 V) sent this surge of electrons, or current pulse, to the rest of the experimental circuit via a R6-58 coaxial cable.

The light guide was a potential a source for lost energy resolution; thus the exterior of the light guide was wrapped and the interfaces on either side were polished carefully. Each interface was first cut square relative to the long axis of the light guide in the upright mill using an end mill bit. Once squared, each face underwent a rigorous sanding and polishing

process, starting with 220 grit sandpaper and working in small increments up to 3000 grit sandpaper. After sanding, a two-part final polishing compound was applied using Kimtech wipes to obtain a final polish on each face.

The entire exterior of the light guide was then wrapped with a two-layer combination of standard kitchen-grade aluminum foil and electrical tape to prevent any light from getting in or out of the light guide. The first layer consisted of aluminum foil carefully wrapped shiny-side in for the full length of the light guide – this layer was initially secured with clear Scotch tape. The aluminum foil was then completely covered with two layers of black electrical tape wrapped in a spiral fashion, such that the only remaining exposed surfaces were the interfaces on either end of the light guide. The tape serves to secure and protect the foil layer, as well as prevent any passage of light into or out of the system.

When attaching the crystal to the light guide interface, a thin layer EJ-550 of silicone optical grease was carefully applied with a gloved finger to the entire surface of both the crystal and light guide parts of the interface. The two parts were pressed firmly into each other and massaged in a circular pattern to ensure full coverage of the interface with the grease. The grease serves to match the refractive indices of the two optical materials, as to not reflect any light traveling from the crystal to the PMT. The interface between the light guide and the 8575 PMT was the same as the NaI crystal-light guide interface. To prevent light from getting in or out of either interface, any seams were wrapped with a layer of aluminum foil, shiny side in to direct any light back into the system. This layer of foil was initially secured by clear scotch tape. To secure the aluminum foil, as well as secure the crystal and PMT to the light guide, black electrical tape was wrapped radially around the junction, connecting each addition to the light guide. Pieces of electrical tape were then placed across each junction for the entire circumference of the junction; these pieces were placed under tension to pull the NaI crystal and PMT into the light guide and maintain the connections between each. A final layer of electrical tape was wrapped in a spiral manner across each junction further secure the connections and ensure no light could pass in either direction. Since a tape-only connection between the NaI crystal and the light guide was not the most durable, the assembly was positioned so gravity held the two together whenever possible.

To test the resolution of the apparatus, energy spectra of ^{22}Na , ^{137}Cs , and ^{60}Co sources were histogrammed using an Amptek MCA 8000A and the circuit in Figure 25. The full width half max (FWHM) was measured at each energy peak. The best energy resolution with the light guide was measured at 14% from the FWHM of the ^{137}Cs 622 KeV peak shown in Figure 26. Unfortunately, the detector/light guide/PMT combination absorbed a great deal of light and had many points where energy resolution could be lost due to an improper connection. This became apparent when the apparatus was taken apart and was no longer able to achieve the same energy resolution once put back together. This reality was the reason for the continued development of the gamma detection apparatus.

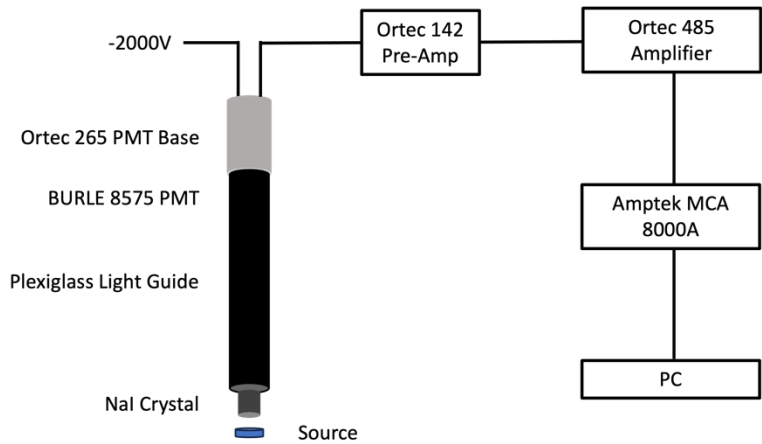


Figure 25. Block diagram of energy spectra test circuit. The MCA outputs a histogram of the gamma ray energies. The full width half max of the energy peaks of each source were taken to determine the energy resolution of the detector.

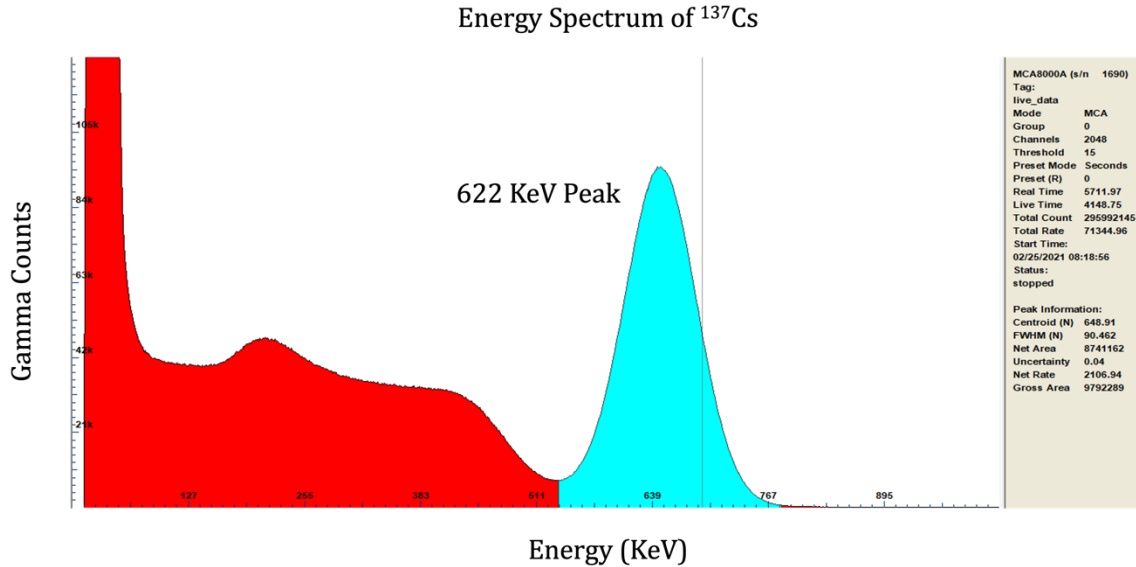


Figure 26. Energy spectrum of ^{137}Cs . The energy resolution of the 622 KeV peak was approximately 14%, which is the lowest value achieved by NaI detector assembly with the light guide.

3.3.2. Silicon Detector

The silicon surface barrier detector (Ortec BA-014-025-1000) was biased to +180 V. It had an active area of 25 mm and a minimum depletion depth of 1 mm. This silicon detector was responsible for measuring beta events in coincidence with the gamma rays, which was necessary to ensure the measurement of only decays where the electron and gamma rays were emitted opposite one another. This forced the measurement of only the two decay modes shown in Figure 11. Unlike the NaI detector, the light guide and PMT are not necessary for the function of the silicon detector. The current pulse in a silicon detector is created when a particle strikes the detector with enough energy to excite electrons from the valence band to the conduction band of the semiconductor. This allows the silicon detector to operate properly within the magnetic field created by the electromagnet.

3.4. Electronics

The electronics are responsible for shaping the pulses from the NaI and Silicon detectors for the digitizer. From the detectors, the current pulses first reached the Ortec 142 pre-amps, in which they were inverted and integrated. From the pre-amps, the pulses traveled to Ortec 454 timing filter amplifiers. These change the shape pulses once again, differentiating and

amplifying the pulses, and adjusting for small differences in time between what should be coincidence pulses. Ensuring the correct timing for coincidence pulses was vital to the experiment; if the pulses from each detector were not close enough in time, they would not trigger the digitizer. The measured pulses must be coincidence pulses to force the situation shown in Figure 11, where the gamma ray was emitted directly opposite the beta particle.

After passing through the timing filter amplifiers, the pulses entered the A and B ports of the SkuTek FemtoDAQ LV-2. The FemtoDAQ combines a fast-digitizing FPGA with an integrated BeagleBone Linux SBC. The FPGA digitized and integrated the incoming pulses, determined whether two pulses were within an acceptable timing range, and recorded the pulse heights and time stamp for each event. The FemtoDAQ recorded coincidence events for equal times with both parallel and antiparallel magnetic field directions.

Chapter 4

CONCLUSIONS

While many of the individual components of the experiment have been assembled and can be tested, the current state of the experiment has not yet allowed for any parity violation measurements. Some components, such as the electromagnet and NaI detector assembly, have yet to undergo final testing before they can be assembled to create the fully functional experiment.

One component of the experiment that requires further development is the NaI detector. The NaI detector assembly was recently disassembled, cleaned, and carefully reassembled to ensure light-tightness and proper optical connection between the crystal, light guide, and PMT. More testing is needed after reassembly to ensure proper energy resolution before the NaI detector assembly is integrated into the rest of the experiment. Once the NaI detector is functioning, the coincidence timing must be measured and adjusted between the NaI and silicon detectors. An improvement that could be made to this assembly in the future would be to replace it with a silicon photomultiplier (SiPM). This would eliminate the need for the light guide, resulting in better energy resolution by eliminating light lost through the interfaces between the crystal, light guide, and PMT.

Another component that must undergo more testing and development is the electromagnet assembly. While the electromagnet has been assembled, proper saturation of the core needs to be confirmed utilizing a teslameter and comparing the magnetic field results to the simulated values. Once this is confirmed, the electromagnet may be integrated into the experimental assembly. Another aspect of the electromagnet that may be developed in the future is a controller to automatically switch the direction of the magnetic field. This will enable extended periods of independent data collection in the future. The controller could also be programmed to switch the direction of the magnetic field at random times to eliminate systematic effects. Another improvement that could be made to the magnet assembly would be to improve the electromagnet design with an integral recess to center

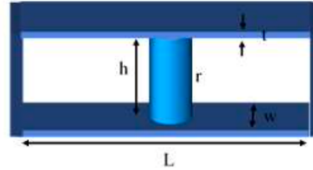
the detectors in the middle of the core, eliminating the need for the 3D printed harnesses. The bobbin core could also be improved with other stronger materials, as the 3D printed bobbin is not very strong and was warped by the force induced by the copper coils.

Once these components are completed, they must be reintegrated into the experiment, the number of coincidence pulses must be measured for equal times with each magnet orientation. The coincidence numbers must be compared, and if the data shows an asymmetry between the number of coincidence events with each magnet orientation, the experiment successfully tests parity violation. If this experiment is successful, it will be the first undergraduate parity violation experiment, and will set a precedent for other undergraduate programs to follow, making parity violation a more universally available phenomenon for physics students worldwide.

Appendix A : SMath File

These SMath calculations show a magnetic field estimate using Ampere's law as seen in Corson & Lorraine 2nd edition, page 408 [15].

Field Estimate for Magnet Design



Constants

$$\mu_0 := (4 \cdot \pi \cdot 10^{-7}) \frac{\text{N}}{\text{A}^2} \quad \text{permeability of free space}$$

Material properties

$$\mu_r := 100 \quad \text{relative permeability} \quad \text{Reasonable for steel?}$$

$$\mu := \mu_r \cdot \mu_0 = 0.0001 \frac{\text{m} \cdot \text{T}}{\text{A}} \quad \text{yoke permeability}$$

Dimensions

$$r := \frac{1.5}{2} \text{ in} = 1.905 \text{ cm} \quad \text{Radius of core}$$

$$L := 6 \text{ in} = 6 \text{ in} \quad \text{Length of magnet yoke}$$

$$t := 0.25 \text{ in} = 0.635 \text{ cm} \quad \text{Thickness of side wall}$$

$$h := 5.635 \text{ cm} - 2 \cdot t = 4.365 \text{ cm} \quad \text{height of cylinder}$$

$$w := 3.5 \text{ in} = 8.89 \text{ cm} \quad \text{Width of yoke}$$

Coil

$$N := 1500 \quad \text{\# of turns}$$

$$E := 24 \text{ V} \quad \text{voltage}$$

$$R := 12.272 \text{ ohm} \quad \text{coil resistance}$$

$$I := \frac{E}{R} = 1.9557 \text{ A} \quad \text{current}$$

$$I := 1 \text{ A}$$

$$P := I^2 \cdot R = 12.272 \text{ W} \quad \text{power}$$

Coil Parameters Calculator

<https://www.daycounter.com/Calculators/Coil-Physical-Properties-Calculator.phtml>

Wire Diameter	0.812	(mm) (See Gauge Table)
Number Turns	1500	(turns)
Bobbin Length	24.6	(mm)
Bobbin Diameter	38	(mm)
Rated DC Current	3	(A)
Turns/Winding	30.296	(Turns/Winding)
Number of Windings	49.512	(Windings)
Coil Diameter	118.408	(mm)
Cross sectional Area	4803.378	(mm ²)
Total Length of Wire	368.527	(m)
Resistance/meter	0.033	(ohms/m)
Resistance	12.272	(ohms)
Voltage at Rated Current	12.272	(V)
Power at Rated Current	12.272	(W)

Magnetic field estimate (see Corson & Lorraine 2nd ed p. 408)

Assumes no flux leakage

$$LY := L + h = 196.05 \text{ mm} \quad \text{length of one side of yoke}$$

$$AY := 2 \cdot t \cdot w = 1129.03 \text{ mm}^2 \quad \text{total area for both sides of yoke}$$

$$A := \pi \cdot r^2 = 1140.0918 \text{ mm}^2 \quad \text{Area of core}$$

$$L := h \quad L = 43.65 \text{ mm} \quad \text{Length of core}$$

$$B := \frac{N \cdot I}{A \cdot \left(\frac{L}{\mu \cdot A} + \frac{LY}{\mu \cdot AY} \right)} = 0.7801 \text{ T}$$

$$\frac{LY}{\mu \cdot AY} = 1.3818 \cdot 10^6 \frac{\text{s}}{\text{A}}$$

$$\frac{L}{\mu \cdot A} = 3.0467 \cdot 10^5 \frac{\text{s}}{\text{A}}$$

Appendix B : FemtoDAQ Python Code

```

#!/usr/bin/python
# parity2.py
# read in detectors from the parity
experiment
# (c) 2020 Houghton College
# Author: M. Yuly
# Created: 2021/02/03
import sys,time, datetime
from FemtoLib import *
### parameters for data capture
OFFSET0 = 0      #offset %
OFFSET1 = 0      #offset %
SIG_POL0 = INVERT      # ADC polarity
SIG_POL1 = INVERT      # ADC polarity
TRIG_POL0 = RISING     # Trigger
polarity
TRIG_POL1 = RISING     # Trigger
polarity
BLR0 = ENABLE          # baseline
restore
BLN_BLOCK0 = 70        # [samples]
baseline blocking period
BLR1 = ENABLE          # baseline
restore
BLN_BLOCK1 = 70        # [samples]
baseline blocking period

PULSE_WIN = 50         # [samples]
pulse height window
SIG_AVG0 = 8           # [samples]
signal averaging time (QDC length)
SIG_AVG1 = 8           # [samples]
signal averaging time (QDC length)
TRIG_AVG0 = 8          # [samples]
trigger averaging time (QDC length)
TRIG_AVG1 = 8          # [samples]
trigger averaging time (QDC length)
PT_DELAY = 4000        # [samples]
post trigger delay
COINCIDENCE = 50       # [samples]
coincidence window
PILEUP = 70            # [samples]
pileup detect window
THRESHOLD0 = 100       # [counts]
trigger threshold
THRESHOLD1 = 2500      # [counts]
trigger threshold
COINCIDENCE_LOG = False # OR
# main routine
#####
# PARSE THE COMMAND LINE
#####
if __name__ == '__main__':
    if len(sys.argv) != 4: # need
a count parameter
        print 'Usage:
parity2.py run_num duration samples'
        print ' run_num =
starting run number'
        print ' duration =
length of run in seconds'
        print ' samples =
number of samples to collect'
        sys.exit()
        # convert run number and catch
any errors
        try:
            run_num =
int(sys.argv[1])
        except:
            print 'Invalid
starting run number'
            sys.exit()
            if (run_num < 0):
                print 'Invalid
starting run number (must be >= 0)'
                sys.exit()
            # convert duration and catch
any errors
            try:
                duration =
int(sys.argv[2])
            except:
                print 'Invalid
duration'
                sys.exit()
                if (duration < 1):
                    print 'Invalid
duration (must be > 0)'
                    sys.exit()
                numSamples = int(sys.argv[3])
                if numSamples > 8192:
                    print 'ERROR: invalid
number of samples (>8192)'
                    sys.exit()
                if numSamples == 8192: # if
all samples, change the value to ALL
                    numSamples = ALL

```

```

#####
# SET UP THE FEMTODAQ
#####
digi = Digitizer() #
create a digitizer object
digi.WaitForReady() # wait
for it to be ready
# read the firmware
fwStr =
digi.GetFirmwareString()
# read the ADctype from the
digitizer
ADctype = digi.IdentifyADC()
digi.InitADC() #
normal mode
#####
# SET UP OUTPUT FILE
#####
outputfilename =
'run_'+str(run_num).rjust(4,'0')+'.dat
'
f = open(outputfilename, 'w')
print >>f, 'Parity2 Experiment
Acquisition'
print>>f, 'Digitizer firmware
revision:', fwStr
print>>f, 'Initializing
ADC',ADctype
print>>f, 'Run
'+str(run_num)+' started at: '+
datetime.datetime.now().strftime("%I:%
M:%S%p on %B %d, %Y")
print 'Parity2 Experiment
Acquisition'
print 'Digitizer firmware
revision:', fwStr
print 'Initializing
ADC',ADctype
print 'Run '+str(run_num)+'
started at: '+
datetime.datetime.now().strftime("%I:%
M:%S%p on %B %d, %Y")
#####
# SET UP DIGITIZER
#####

digi.SetChannelSignalPolarity(0,SIG_PO
L0)

digi.SetChannelSignalPolarity(1,SIG_PO
L1)

digi.SetChannelTriggerEdge(0,TRIG_POLO
)

digi.SetChannelTriggerEdge(1,TRIG_POL1
)
if BLR0:
digi.EnableChannelBaselineRestore(0)
else:
digi.DisableChannelBaselineRestore(0)
if BLR1:
digi.EnableChannelBaselineRestore(1)
else:
digi.DisableChannelBaselineRestore(1)

digi.SetChannelBaselineBlocking(0,BLN_
BLOCK0)

digi.SetChannelBaselineBlocking(1,BLN_
BLOCK1)
# set the signal averaging
time for each channel

digi.SetChannelSignalAveragingTime(0,S
IG_AVG0)

digi.SetChannelSignalAveragingTime(1,S
IG_AVG1)
# set the trigger averaging
time for each channel

digi.SetChannelTriggerAveragingTime(0,
TRIG_AVG0)

digi.SetChannelTriggerAveragingTime(1,
TRIG_AVG1)
# set the trigger level

digi.SetChannelTriggerThreshold(0,THRE
SHOLD0)

digi.SetChannelTriggerThreshold(1,THRE
SHOLD1)
# set the coincidence window

digi.SetCoincidenceWindow(COINCIDENCE)

digi.SetCoincidenceLogic(COINCIDENCE_L
OG)
# set the pileup detect window

digi.SetPileupDetectWindow(PILEUP)
# set the post trigger delay

```

```

digi.SetPostTriggerDelay(PT_DELAY)
    digi.Initialize(False) #
Initialize w/o ADC init
    time.sleep(0.1) # need
> 1ms to initialize
    digi.EnableChannelTrigger(0)
    digi.EnableChannelTrigger(1)
    time.sleep(0.1)
    # start a new capture
    digi.StartCapture()
    time.sleep(0.2)
    events = 0
    start = time.time()
#start time (sec)
    last = time.time()
    while (last-start < duration)
:
    digi.StartCapture()
    #time.sleep(0.2)

    digi.WaitForTrigger() # wait
for a trigger to occur
    #print 'Triggered'
    now = time.time()-start
    #time.sleep(0.1)
    data0 =
digi.GetSamples(0,numSamples)
    data1 =
digi.GetSamples(1,numSamples)
    max0 = 0
    imax0 = -1
    for i in
range(PT_DELAY,PT_DELAY+400):
    #print>>f, data0[i]
    if data0[i]>max0:
        max0 = data0[i]
        imax0 = i
    max1 = 0
    imax1 = -1
    for i in
range(PT_DELAY,PT_DELAY+400):
    #print>>f, data1[i]
    if data1[i]>max1:
        max1 = data1[i]
        imax1 = i
    last = time.time()
    print now, imax0, max0,
imax1, max1
    print>>f, now, imax0, max0,
imax1, max1
    #print 'num of samples: 0 = %d
in 1 = %d' % (len(data0),len(data1))
    # write to output file
    #print>>f, '\n Channel 0'

#print '\n Channel 0'
#for cc0 in data0:
    #print>>f, cc0
    #print cc0
#print>>f, '\n Channel 1'
#print '\n Channel 1'
#for cc1 in data1:
    #print>>f, cc1
    #print cc1

f.close()
digi.DisableChannelTrigger(0)
digi.DisableChannelTrigger(1)
digi.close() #
release the SPI lines
    print 'Done'
public@L20003:~/parity$ cp parity2
parity2.py parity2_analyze.C
public@L20003:~/parity$ cp parity2.py
cp: missing destination file operand
after 'parity2.py'
Try 'cp --help' for more information.
public@L20003:~/parity$ cat parity2.py
| clipboard
Command 'clipboard' not found, did you
mean:
    command 'xclipboard' from deb x11-
apps
Try: sudo apt install <deb name>
public@L20003:~/parity$ cat parity2.py
| xclip
Command 'xclip' not found, but can be
installed with:
sudo apt install xclip
public@L20003:~/parity$ sudo apt
install xclip
Reading package lists... Done
Building dependency tree
Reading state information... Done
The following NEW packages will be
installed:
    xclip
0 upgraded, 1 newly installed, 0 to
remove and 0 not upgraded.
Need to get 17.5 kB of archives.
After this operation, 52.2 kB of
additional disk space will be used.
0% [Connecting to
archive.ubuntu.com]^C
public@L20003:~/parity$ cat parity2.py
#!/usr/bin/python
# parity2.py
# read in detectors from the parity
experiment
# (c) 2020 Houghton College
# Author: M. Yuly

```

```

# Created: 2021/02/03
import sys,time, datetime
from FemtoLib import *
### parameters for data capture
OFFSET0 = 0      #offset %
OFFSET1 = 0      #offset %
SIG_POL0 = INVERT      # ADC polarity
SIG_POL1 = INVERT      # ADC polarity
TRIG_POL0 = RISING     # Trigger
polarity
TRIG_POL1 = RISING     # Trigger
polarity
BLR0 = ENABLE          # baseline
restore
BLN_BLOCK0 = 70        # [samples]
baseline blocking period
BLR1 = ENABLE          # baseline
restore
BLN_BLOCK1 = 70        # [samples]
baseline blocking period
PULSE_WIN = 50         # [samples]
pulse height window
SIG_AVG0 = 8           # [samples]
signal averaging time (QDC length)
SIG_AVG1 = 8           # [samples]
signal averaging time (QDC length)
TRIG_AVG0 = 8          # [samples]
trigger averaging time (QDC length)
TRIG_AVG1 = 8          # [samples]
trigger averaging time (QDC length)
PT_DELAY = 4000        # [samples]
post trigger delay
COINCIDENCE = 50       # [samples]
coincidence window
PILEUP = 70            # [samples]
pileup detect window
THRESHOLD0 = 100       # [counts]
trigger threshold
THRESHOLD1 = 2500      # [counts]
trigger threshold
COINCIDENCE_LOG = False # OR
# main routine
#####
# PARSE THE COMMAND LINE
#####
if __name__ == '__main__':
    if len(sys.argv) != 4: # need
a count parameter
        print 'Usage:
parity2.py run_num duration samples'
        print ' run_num =
starting run number'
        print ' duration =
length of run in seconds'
        print ' samples =
number of samples to collect'
        sys.exit()
        # convert run number and catch
any errors
        try:
            run_num =
int(sys.argv[1])
        except:
            print 'Invalid
starting run number'
            sys.exit()
            if (run_num < 0):
                print 'Invalid
starting run number (must be >= 0)'
                sys.exit()
            # convert duration and catch
any errors
            try:
                duration =
int(sys.argv[2])
            except:
                print 'Invalid
duration'
                sys.exit()
                if (duration < 1):
                    print 'Invalid
duration (must be > 0)'
                    sys.exit()
                numSamples = int(sys.argv[3])
                if numSamples > 8192:
                    print 'ERROR: invalid
number of samples (>8192)'
                    sys.exit()
                    if numSamples == 8192: # if
all samples, change the value to ALL
                        numSamples = ALL
                        #####
                        # SET UP THE FEMTODAQ
                        #####
                        digi = Digitizer() #
create a digitizer object
                        digi.WaitForReady() # wait
for it to be ready
                        # read the firmware
                        fwStr =
digi.GetFirmwareString()
                        # read the ADctype from the
digitizer
                        ADctype = digi.IdentifyADC()
                        digi.InitADC() #
normal mode
                        #####
                        # SET UP OUTPUT FILE
                        #####

```

```

        outputfilename =
'run_'+str(run_num).rjust(4,'0')+'.dat
'
        f = open(outputfilename, 'w')
        print >>f, 'Parity2 Experiment
Acquisition'
        print>>f, 'Digitizer firmware
revision:', fwStr
        print>>f, 'Initializing
ADC',ADCTYPE
        print>>f, 'Run
'+str(run_num)+' started at: '+
datetime.datetime.now().strftime("%I:%
M:%S%p on %B %d, %Y")
        print 'Parity2 Experiment
Acquisition'
        print 'Digitizer firmware
revision:', fwStr
        print 'Initializing
ADC',ADCTYPE
        print 'Run '+str(run_num)+'
started at: '+
datetime.datetime.now().strftime("%I:%
M:%S%p on %B %d, %Y")
        #####
        # SET UP DIGITIZER
        #####

digi.SetChannelSignalPolarity(0,SIG_PO
L0)

digi.SetChannelSignalPolarity(1,SIG_PO
L1)

digi.SetChannelTriggerEdge(0,TRIG_POL0
)

digi.SetChannelTriggerEdge(1,TRIG_POL1
)
        if BLR0:

digi.EnableChannelBaselineRestore(0)
        else:

digi.DisableChannelBaselineRestore(0)
        if BLR1:

digi.EnableChannelBaselineRestore(1)
        else:

digi.DisableChannelBaselineRestore(1)

digi.SetChannelBaselineBlocking(0,BLN_
BLOCK0)

digi.SetChannelBaselineBlocking(1,BLN_
BLOCK1)
        # set the signal averaging
time for each channel

digi.SetChannelSignalAveragingTime(0,S
IG_AVG0)

digi.SetChannelSignalAveragingTime(1,S
IG_AVG1)
        # set the trigger averaging
time for each channel

digi.SetChannelTriggerAveragingTime(0,
TRIG_AVG0)

digi.SetChannelTriggerAveragingTime(1,
TRIG_AVG1)
        # set the trigger level

digi.SetChannelTriggerThreshold(0,THRE
SHOLD0)

digi.SetChannelTriggerThreshold(1,THRE
SHOLD1)
        # set the coincidence window

digi.SetCoincidenceWindow(COINCIDENCE)

digi.SetCoincidenceLogic(COINCIDENCE_L
OG)
        # set the pileup detect window

digi.SetPileupDetectWindow(PILEUP)
        # set the post trigger delay

digi.SetPostTriggerDelay(PT_DELAY)
        digi.Initialize(False) #
Initialize w/o ADC init
        time.sleep(0.1) # need
> 1ms to initialize
        digi.EnableChannelTrigger(0)
        digi.EnableChannelTrigger(1)
        time.sleep(0.1)
        # start a new capture
        digi.StartCapture()
        time.sleep(0.2)
        events = 0
        start = time.time()
        #start time (sec)
        last = time.time()
        while (last-start < duration)
:
                digi.StartCapture()

```

```

        #time.sleep(0.2)
        digi.WaitForTrigger() # wait
for a trigger to occur
        #print 'Triggered'
        now = time.time()-start
        #time.sleep(0.1)
        data0 =
digi.GetSamples(0,numSamples)
        data1 =
digi.GetSamples(1,numSamples)
        max0 = 0
        imax0 = -1
        for i in
range(PT_DELAY,PT_DELAY+400):
            #print>>f, data0[i]
            if data0[i]>max0:
                max0 = data0[i]
                imax0 = i
        max1 = 0
        imax1 = -1
        for i in
range(PT_DELAY,PT_DELAY+400):
            #print>>f, data1[i]
            if data1[i]>max1:
                max1 = data1[i]

```

```

        imax1 = i
        last = time.time()
        print now, imax0, max0,
imax1, max1
        print>>f, now, imax0, max0,
imax1, max1
        #print 'num of samples: 0 = %d
in 1 = %d' % (len(data0),len(data1))
        # write to output file
        #print>>f, '\n Channel 0'
        #print '\n Channel 0'
        #for cc0 in data0:
            #print>>f, cc0
            #print cc0
        #print>>f, '\n Channel 1'
        #print '\n Channel 1'
        #for cc1 in data1:
            #print>>f, cc1
            #print cc1
        f.close()
        digi.DisableChannelTrigger(0)
        digi.DisableChannelTrigger(1)
        digi.close() #
        release the SPI lines
        print 'Done'

```

Appendix C : Analysis Codes

```

// (c) 2020 Houghton College
// Author: M. Yuly
// Created: 2021/02/03

#include <iostream>

//
=====
// Subroutine to read data from run
file, fill histograms and ntuple
//
=====
void read_file(TString fname, TH1F *h0,
TH1F *h1, TH2F *h01, TH1F *ht, TNtuple
*ntuple, float offset) {

char cline[256];
// input line buffer

// data from Femtodaq
Int_t tadc0, adc0, tadc1, adc1;
float timestamp;

printf("Opening input file: %s \n ",
fname.Data());
ifstream in;
in.open(fname.Data());

// Read in the first 10 comment lines
for (int i=1; i<13; i++) {
    in.getline(cline,256);
    printf("line %d %s
\n",i,cline);
    //cout<<"line"<<i<<":
"<<cline<<endl;

}

// number of data lines read in from
each file
Int_t nlines = 0;

// Read in data and fill histograms and
ntuple
do {
    in >>
timestamp>>tadc0>>adc0>>tadc1>>adc1;
    //printf("in fail =
%d\n",in.fail());
    if (in.fail()) break;

    if (nlines < 5) printf("%d
time=%10.4f tadc0=%d adc0=%d tadc1=%d
adc1=%d
\n",in.good(),timestamp,tadc0,adc0,tadc
1, adc1);

    h0->Fill(adc0); //
hist dE
    h1->Fill(adc1); //
hist E
    h01->Fill(adc1,adc0); // dE
vs E

    ht->Fill( tadc0-tadc1 );

    ntuple->Fill(timestamp,tadc0,
adc0, tadc1, adc1);

    nlines++;

} while(!in.eof());

printf(" found %d points\n",nlines);
//printf("start=%ld \n",start);
//printf("time=%ld adc0=%d adc1=%d
\n",timestamp,adc0,adc1);

in.close();
}

//
=====
// Main
//
=====
void parity2_analyze(TString
fname="test") {
// read in and analyze data from
parity.py
// created: 07/2016 Mark Yuly
// modified: 01/19/2017 Mark Yuly
read in data saved by new FemtoDAQ FPGA
program

// ===== USER SETTABLE VALUES
=====

```

```

// length of run in seconds
Int_t run_length = 1;

// size of time bin (ns)
Int_t time_bin_size = 10;

//
=====
=====

TString run_file;           // list
of run file names to process
int numlist;               //
number of files to process
float offset;              //
offset for each run
int in_run_num;           // run number
to input
char buffer[100];         //
temporary buffer
char last_buffer[100];    //
temporary buffer of last item processed

char cline[256];
// input line buffer
char str[30];
// char string buffer

printf("Opening run run file: %s\n",
fname.Data());

// create the histograms
TString root_name = fname;
root_name.Append(".root");
TFile *f = new
TFile(root_name,"RECREATE");
TH1F *h0 = new
TH1F("h0","ADC0_spectrum",10000,0,9999)
;
h0->SetFillColor(0);
TH1F *h1 = new
TH1F("h1","ADC1_spectrum",10000,0,9999)
;
h1->SetFillColor(0);
TH2F *h01 = new TH2F("h01","ADC0 vs
ADC1",1000,0,9999,1000,0,9999);
h01->SetFillColor(0);
TH1F *ht = new TH1F("ht","time
difference",400,0.,499.);
ht->SetFillColor(0);

// create the root tree for output root
file

TNtuple *ntuple = new
TNtuple("ntuple","data from ascii
file","timestamp,adc0,adc1");

//Either open a single run file, or
loop through a list of run files
if (fname(0,3)=="run") {
// single run file
printf("Opening run run file:
%s\n", fname.Data());
offset = 0;
read_file(fname, h0, h1, h01,
ht, ntuple, offset);
printf(" File opened and read
successfully.\n");
}
else {
printf("Opening run list file:
%s\n", fname.Data());
ifstream in_list;
in_list.open(fname.Data());

// number of data lines read in
from each file
numlist = 0;

// Read in the file names and
offsets
do {
in_list >> offset>>in_run_num;

sprintf(buffer,"run_%04d.dat",in_run_num);

//cout<<offset<<in_run_num<<endl;
run_file=buffer;

//printf("[%s]",run_file.Data());
//if (numlist < 50)
printf("%d %s %4.2f
\n",in_list.good(),run_file.Data(),offs
et);

if (buffer[7] !=
last_buffer[7]) read_file(run_file,
h0, h1, h01, ht, ntuple, offset);
numlist++;
strcpy(last_buffer,
buffer);
} while (!in_list.eof());

printf(" Found %d runs in
list\n",numlist);
}

// Show histograms of dE E and 2D

```

```

TCanvas *c1 = new
TCanvas("c1", fname.Data(), 200, 10, 800, 60
0);
c1->SetFillColor(0);

TPad *pad1 = new
TPad("pad1", "ADC0", 0.03, 0.62, 0.50, 0.92,
21);
pad1->SetFillColor(0);
TPad *pad2 = new
TPad("pad2", "ADC1", 0.51, 0.62, 0.98, 0.92,
21);
pad2->SetFillColor(0);
TPad *pad3 = new TPad("pad3", "ADC0 vs
ADC1", 0.03, 0.02, 0.97, 0.57, 21);
pad3->SetFillColor(0);
pad1->Draw();
pad2->Draw();
pad3->Draw();

pad1->SetBottomMargin(0.15);
pad1->SetLeftMargin(0.14);
pad2->SetBottomMargin(0.15);
pad2->SetLeftMargin(0.14);

h0->GetXaxis()->SetTitle("dE (ADC0)");
h0->GetXaxis()->SetLabelSize(0.06);
h0->GetXaxis()->SetTitleSize(0.06);
h0->GetYaxis()->SetTitle("Number of
counts");
h0->GetYaxis()->SetLabelSize(0.06);
h0->GetYaxis()->SetTitleSize(0.06);
h0->GetYaxis()->SetTitleOffset(1.1);

h1->GetXaxis()->SetTitle("E (ADC1)");
h1->GetXaxis()->SetLabelSize(0.06);
h1->GetXaxis()->SetTitleSize(0.06);
h1->GetYaxis()->SetTitle("Number of
counts");
h1->GetYaxis()->SetLabelSize(0.06);
h1->GetYaxis()->SetTitleSize(0.06);
h1->GetYaxis()->SetTitleOffset(0.8);

h01 -> SetYTitle("dE (ADC0)");
h01->GetYaxis()->SetTitleOffset(0.9);
h01 -> SetXTitle("E (ADC1)");
//h01->GetYaxis()->SetRange(1000,
2200);

//h01->GetXaxis()->SetRangeUser(300,
2000.);

pad1->cd();
h0->Draw();
pad2->cd();
h1->Draw();
pad3->cd();
h01->Draw();
pad3->Draw();
c1->Update();

//Show histogram vs time and fit
histogram
TCanvas *c2 = new
TCanvas("c2", fname.Data(), 200, 10, 800, 60
0);

gPad->SetBottomMargin(0.15);
ht->GetYaxis()->SetTitle("Number of
counts");
ht->GetXaxis()->SetTitle("time (s)");
gStyle->SetErrorX(0.0001);
ht->SetLineColor(kBlack);
ht->SetMarkerStyle(20);
ht->SetFillColor(kGreen);
ht->GetXaxis()->SetLabelSize(0.03);
ht->GetXaxis()->SetTitleSize(0.03);
ht->GetYaxis()->SetLabelSize(0.03);
ht->GetYaxis()->SetTitleSize(0.03);
ht->GetYaxis()->SetTitleOffset(1.7);

ht->GetYaxis()->SetRangeUser(0, 50);

ht->Draw("E1");
gPad->Draw();

c2->Update();

// write the histogram and ntuples to
root file
f->Write();

```

References

-
- [1] A. Wroblewski, ACTA Phys. Pol. B **39**, 251 (2008).
- [2] H. Weyl, Zeit. Phys. **56**, 330 (1929).
- [3] W. Pauli, Handbuch der Physik **24**, 185 (1933).
- [4] R.W. Birge, J. Peterson, D.H. Stork, M.N. Whitehead, Phys. Rev. **100**, 430 (1955); V. Fitch, R. Motley, Phys. Rev. **101**, 496 (1955); L.W. Alvarez, F.S. Crawford, M.L. Good, M.L. Stevenson, Phys. Rev. **101**, 503 (1955).
- [5] R.P. Feynman, *Surely You're Joking, Mr. Feynman! The Adventures of a Curious Character as told to Ralph Leighton*, (W.W. Norton & Company, New York–London, 1985), p. 247–248.
- [6] T.D. Lee, C.N. Yang, Phys. Rev. **104**, 254 (1956).
- [7] H. Frauenfelder, E.M. Henley, *Nuclear and Particle Physics*, (Benjamin, Reading, Mass., 1975), p. 389.
- [8] C. Wu et al., Phys. Rev. **105**, 1413 (1957).
- [9] M. Goldhaber et al., Phys. Rev. **106**, 826 (1957).
- [10] M. Goldhaber et al., Phys. Rev. **109**, 1015 (1957).
- [11] H. Schopper, Nuc Phys **3**, 158 (1958).
- [12] A. Lundby, A. P. Patro, J. P. Stroot, Nuovo Cimento **6**, 745 (1957).
- [13] *Live Chart of Nuclides (2024) Livechart - table of nuclides - nuclear structure and decay data*. Available at: <https://www-nds.iaea.org/relnsd/vcharthtml/VChartHTML.html> (Accessed: 25 April 2024).
- [14] Chubar O, Elleaume P, Chavanne J. A three-dimensional magnetostatics computer code for insertion devices. J Synchrotron Radiat. 1998 May 1;5(Pt 3):481-4. doi: 10.1107/S0909049597013502. Epub 1998 May 1. PMID: 15263552.
- [15] D. Corson, P. Lorraine, *Electromagnetic Fields and Waves*, 2nd ed. (W. H. Freeman and Co., New York, 1970), p. 407-409.